Chapter PP

PETROPHYSICAL PROPERTIES

by Philip H. Nelson[1]

in The Oil and Gas Resource Potential of the 1002 Area, Arctic National Wildlife Refuge, Alaska, by ANWR Assessment Team, U. S. Geological Survey Open File Report 98-34.

1999

[1] U.S. Geological Survey, MS 939, Denver, CO 80225

TABLE OF CONTENTS

PP1h	Cumulative percentage of porosity in Kemik Sandstone, from well logs.
PP1i.	Cumulative percentage of porosity in Canning Formation, from well logs.
PP1j	Cumulative percentage of porosity in Sagavanirktok Formation, from well logs.
PP2	Porosity versus vitrinite reflectance, Canning Formation
PP3	Porosity versus vitrinite reflectance, Sagavanirktok Formation
PP4	Porosity and vitrinite reflectance variations with depth.
PP5a	Capillary pressure by mercury injection, logarithmic scale, Sabbath Creek Formation.
PP5b	Capillary pressure by mercury injection, logarithmic scale, Lisburne Formation
PP5c	Capillary pressure by mercury injection, logarithmic scale, Kekiktuk Formation.
PP5d	Capillary pressure by mercury injection, logarithmic scale, Ivishak Formation.
PP5e	Capillary pressure by mercury injection, logarithmic scale, Kemik Sandstone.
PP5f	Capillary pressure by mercury injection, logarithmic scale, Canning Formation
PP5g	Capillary pressure by mercury injection, logarithmic scale, Sagavanirktok Formation
PP5h	Capillary pressure by mercury injection, logarithmic scale, Sagavanirktok Formation
PP5i	Capillary pressure by mercury injection, logarithmic scale, Shublik Formation
PP6a	Capillary pressure by mercury injection, linear scales, Lisburne Formation.
PP6b	Capillary pressure by mercury injection, linear scales, Kekiktuk Formation
PP6c	Capillary pressure by mercury injection, linear scales, Ivishak Formation
PP6d	Capillary pressure by mercury injection, linear scales, Kemik Sandstone.
PP6e	Capillary pressure by mercury injection, linear scales, Canning Formation.
PP6f	Capillary pressure by mercury injection, linear scales, Sagavanirktok Formation
PP7	Partitioning of a shaly sand into solid and pore space fractions.
PP8	Water saturation in Prudhoe Bay Field, by area and zone
PP9	Water saturation versus porosity at 300 psi mercury injection pressure.
PP10	Water saturation versus porosity, Kekiktuk Formation.
PP11	Formation velocities and standard deviations, from well logs.
PP12	Average density by formation, from well logs.

ABSTRACT

Physical property data are compiled from wells immediately west and north of the Arctic National Wildlife Refuge (ANWR), and from tests of additional core and surface samples acquired during the assessment project within and adjacent to ANWR. Net thicknesses of reservoir-prone rocks calculated from gamma-ray logs are used to determine net-to-gross ratios for ten formations. Porosity distributions in the same intervals are calculated from well logs and made available for assessing individual plays. Examination of porosity and vitrinite reflectance data shows that an existing statistical model is adequate for predicting porosity trends with depth for some lithologies within ANWR. Capillary pressure data obtained from core plugs and surface samples help substantiate the use of a constant-water-volume-fraction model to compute water saturation. Velocity data extracted from sonic logs aid the interpretation of seismic data, and density data extracted from density logs aid the interpretation of gravity data.

INTRODUCTION

The assessment procedure requires an estimate of the hydrocarbon volume in place, which is the product of $\varphi(1-S_w)Ah(TF)$ where φ is porosity, S_w is water saturation, A is area of closure, h is mean reservoir net thickness, and TF is trap fill. This report deals with data and methods for estimating h, φ, and S_w.

In play assessment, an estimate of gross thickness may be available from seismic or from geological knowledge, in which case the net thickness can be readily determined if the assessor knows the approximate net-to-gross thickness ratio. We establish the net-to-gross ratio for ten formations using well logs to determine the net thickness.

Porosity can be estimated from core tests and from well logs; this report summarizes porosity data from wells immediately west and north of ANWR (Fig. AO3). Porosity data from North Slope petroleum reservoirs are summarized by Nelson and Bird (Chap. FP). Here we also evaluate a method of predicting porosity on the basis of thermal maturity, which is expressed in terms of vitrinite reflectance.

Water saturation was not calculated from logs in wells adjacent to ANWR, because there were few petroleum reservoirs encountered by the drill (an

exception is the Thomson sand). Instead we examine the validity of a rule-of-thumb method for calculating water saturation which relies upon the near constancy of the water volume fraction in petroleum reservoirs. This simple algorithm appears adequate for our assessment purposes. Its adoption does require that water saturation be computed from porosity; hence water saturation is treated as a dependent variable and is not sampled from a distribution function as is porosity.

Velocity and density data were determined from log and core data in support of seismic and gravity interpretations, and are tabulated and graphed in this report.

While this report describes the procedures used to extract information from the well log and core data, the compilation and availability of these data are described by Nelson and others (Chap. WL). Other aspects of reservoir quality are discussed by Nelson and Bird (Chap. FP).

NET AND GROSS THICKNESS

Each formation where porosity was to be computed was inspected to determine the presence of sand from all logs and core data and to determine an appropriate indicator of sand occurrences. Most often the gamma-ray log was adequate for the purpose, although the cutoff level (API units), as determined by visual inspection, varies somewhat from formation to formation. The total footage in which the gamma-ray criterion (such as gamma ray < 45 API units) was satisfied was recorded as net thickness.

Average gross and net thicknesses are posted in Table PP1. Gross thickness is usually the difference between top and bottom of a formation. (Gross thickness of each formation in each well is given in Table WL6.) If a formation was only partially penetrated, or if well logs were incomplete within a formation, then gross thickness is equal to the section penetrated or the section logged.

For assessment purposes, an assessor can pick the expected mean value of vertical thickness of a trap from stratigraphic and seismic considerations. For that thickness, the assessor then applies the net/gross ratio from column five of Table PP1, if that ratio is deemed representative for a play.

For plays incorporating Ellesmerian section, the expected thickness of non-

reservoir formations must first be removed. Table PP2 gives average gross thicknesses of all Ellesmerian formations, both reservoir and non-reservoir (gross thickness values differ between Table PP1 and PP2 because the number of wells differs). It is possible to estimate the net reservoir thickness for different scenarios of Ellesmerian occurrences using Table PP1 and PP2, although one first must assume a net-to-gross ratio for the Lisburne Group.

POROSITY

Porosity, permeability, and saturation from core measurements. Table PP3 lists permeability, porosity, and oil saturation for individual samples, by well, with formation and depth also listed. These measurements are presumed to have been made at ambient conditions. Columns 7 through 9 give average porosity, standard deviation, and number of points in the average, for each formation in each well. If the data were known (from inspection of well logs) to vary within a formation, then averaging was carried out over subsections of that formation (see Kekiktuk samples in Badami 1). Other porosity data, obtained on samples cut by USGS investigators, can be found in Table PP4.

Porosity determinations from well logs. Porosity was determined within those intervals satisfying the criterion for net sand. Porosity was computed from well logs in one of the three following ways, depending upon log availability and lithology:

1) From the density log, $\varphi_D = (\rho_{ma}-\rho) / (\rho_{ma}-\rho_{fl})$, where the fluid density $\rho_{fl} = 1$ and the grain (matrix) density ρ_{ma} is obtained from core measurements (Table PP5). If the caliper and density logs indicated that density log quality was not compromised by rough hole conditions, then the density log was used to compute porosity, with a value of grain density assigned to each formation in accordance with Table PP5.

2) From the sonic log, $\varphi_S = (\Delta t - \Delta t_{ma}) / (\Delta t_{fl} - \Delta t_{ma})$, where the travel time in a zero-porosity solid, Δt_{ma}, was usually taken to be 55 μs/ft, and the travel time in fluid, Δt_{fl}, was taken to be 189 μs/ft. In cases where the density log was missing or of poor quality, then the sonic log was used to compute porosity. Porosity computed from the sonic log has a high uncertainty within the Sagavaniroktok and Canning Formations due to lack of compaction.

3) To determine porosity from a neutron-density crossplot, the algorithm encoded in software was used. The neutron-density method was used in basement carbonates, in the Lisburne Formation, and in the Thomson Formation, where the grain density varies substantially due to sand-calcite-dolomite mineralogical variations. In one well, a sidewall epithermal neutron was available and was used for the porosity determination.

No attempt was made to correct the computed porosity values for clay content or for gas content.

Cumulative distribution functions of porosity. Histograms and cumulative distributions of porosity, based either upon core or computed from well logs by one of the methods described above, were plotted for individual formations in selected wells. Values were then extracted at seven points from the cumulative distributions: 0, 5, 25, 50, 75, 95, and 100%. The 0 and 100% values represent the minimum and maximum of the range, and the 50% value is the median value. The 25% value, designated φ_{25}, indicates that 25% of the population have a value less than φ_{25}, or that 75% of the population have a value greater than φ_{25}. The resulting distributions are plotted in Figs. PP1a through PP1j for the 10 formations determined to have reservoir potential.

Vitrinite reflectance as a function of depth. Vitrinite reflectance data were assembled from data files compiled by Johnsson and others (1993) and from public well files. A linear function for R_o with respect to depth was fit by least-squares regression, $\ln(R_o) = \ln(a) + bz$, where z is depth in feet, and $\ln(a)$ and b are regression coefficients, as given by Bird (Chap. VR). To compute a value of R_o in each formation, the value of z was taken to be the mid-point of the formation. Where the average porosity was determined over an interval less than formation thickness (e.g., because of incomplete log coverage), the vitrinite reflectance was computed for the mid-point of that same interval, rather than at the formation mid-point. In this way, a value of R_o is associated with each porosity distribution.

Porosity as a function of vitrinite reflectance. Following the method of Schmoker and Hester (1990), the cumulative distributions of porosity were plotted against vitrinite reflectance (Figs. PP2 and PP3). Schmoker and Hester determined statistically that roughly one-half of the variance in porosity could be accounted for by thermal maturity, as measured by

vitrinite reflectance. The use of vitrinite reflectance as a predictor of porosity is believed to be an improvement over the use of depth as a predictor. Figures PP2 and PP3 show the data from wells adjacent to ANWR for the Canning and Sagavanirktok Formations, plotted against the Schmoker-Hester fits for the fifth through ninety-fifth percentiles (we have added the 0 and 100 percentile lines). The A and B coefficients for the Schmoker-Hester regression equations are given in Table PP6. The data for these two formations match the Schmoker-Hester distribution reasonably well.

For other formations (not shown), the fit is less satisfactory. It is better to use mean values of the actual porosity distributions for the basement rocks and the Lisburne Formation, without any dependence upon vitrinite reflectance whatsoever.

To illustrate the dependence of R_o and porosity with depth, two cases are plotted in Fig. PP4: Ro_{NW} uses *a,b* coefficients appropriate for the undeformed area northwest of the Marsh Creek anticline within ANWR, and Ro_{SE} uses coefficients appropriate for the deformed area southeast of the Marsh Creek anticline. The rate of increase of vitrinite reflectance with depth (*b*) is taken from groups of wells closest to these two areas, and the surface value (*a*) is determined from the map of vitrinite reflectance values from surface samples (Chap. VR). As a consequence, the rate of decrease of porosity with depth and surface values of porosity likewise depend upon the choice of the vitrinite reflectance characteristics. Note the exponential decline of porosity with depth. It should be mentioned that a compaction factor is built into the predictor because the Schmoker-Hester equations have been compared with porosity values derived from well logs.

Application. In practice, the porosity dependence upon R_o and hence upon depth, as depicted in Fig. PP4, was used as a guideline, and in conjunction with other considerations, in establishing the Play porosity distributions. It should be remembered that the porosity distributions for the Plays must encompass the values expected for the average values of individual prospects within Plays, whereas porosity distributions from well logs or from the Schmoker-Hester equations encompass the full range of values expected for individual fields.

In other words, the porosity distributions adopted for the assessment of a play (Chap. RS) will not necessarily mimic the porosity distributions found

in nearby wells. The assessor must judge whether or not the well-based porosity values are representative of the lithologies envisioned for the play, and adjust accordingly.

CAPILLARY PRESSURE BY THE MERCURY INJECTION METHOD

At the request of the USGS, capillary pressure measurements were performed by Poro-Technology (J. Neasham) of Houston, Texas. Before testing, samples were dried at 90 degrees C. Mercury was injected into a sample using a Micromeritics Autopore II 9220 testing machine with a high pressure capacity of 60,000 psi. Initial injection pressures were about 1.5 psi. Plots of mercury injection pressure versus pore volume occupied by mercury are presented by formation (Figs. PP5a through PP5i). Locations of surface samples are described by Schenk and others, Chap. FS, and cored intervals from which plugs were taken are shown in plates of Chap. WL. To accomodate the very large range in capillary pressure, pressure is scaled logarithmically in Figs. PP5a through PP5i. This scale has the disadvantage of obscuring the capillary pressure behavior at realistic reservoir pressures. So, a subset of the samples are presented on linear scales in Figs. PP6a through PP6f.

Characteristics of good reservoir quality are low entry pressure and a long plateau of nearly constant capillary pressure as the sample fills with mercury. A long continuous plateau shows that a large fraction of pore space is interconnected and is of uniform pore throat size. The best examples are from the Sagavanirktok Formation (Fig. PP5g): three samples (95-21, 95-22, and 96-153) dispay low entry pressures of less than 10 psi and have a plateau extending from 0 to 60% of pore space.

How do capillary pressure curves correspond to pore space? A shaly sand model (Fig. PP7) is probably representative of the Canning Formation, and to a lesser extent (with diminishing clay content) is representative of the Sagavanirktok and Ivishak Formations. Both clay-bound and capillary water occupy pore space accessible only at high injection pressures through small pore throats. Three samples from the Kekiktuk Formation (Figs. PP5c and PP6b) illustrate the relation between capillary pressure and pore content. The three samples have low entry pressures ranging from 7 to 11 psi. Pore space is of uniform size and is well connected, as demonstrated by the plateau. Choosing 300 psi as a cutoff, the irreducible water saturation values, S_{wi}, are 6, 12, and 16% of pore space. The porosity

invaded by mercury is equivalent to the producible porosity φ_p of Fig. PP7, and is equal to 0.94, 0.88, and 0.84 of total porosity of the respective samples.

The conversion from capillary pressure measured by mercury injection to a saturation profile in a reservoir is a function of oil-water surface tension and density difference between formation water and oil (e.g. Jennings, 1987). However, density and oil-water surface tension depends upon oil type, temperature, and other factors which vary among reservoirs. We chose a value of 300 psi as a representative pressure for attaining irreducible water saturation in a reservoir rock; it could correspond to a height of one hundred to many hundreds of feet of oil column. (A value of 265 psi was adopted by Dodge and others (1996) for a 100-foot oil column.) Values of S_{wi} were read from the capillary pressure curves at 300 psi, and entered into Table PP4 for samples sufficiently permeable that $S_{wi}<1.0$ at 300 psi.

WATER SATURATION

In good reservoir rock, the capillary pressure curve exhibits a long flat plateau and a sharp knee where the curve changes from nearly flat to nearly vertical (see three leftmost curves in Fig. PP6f). Within the vertical portion of the curve, large changes in pressure are required to produce small changes in saturation. The water saturation in this portion of the curve is called the *irreducible water saturation*, S_{wi}. In good quality reservoir rock, pressure becomes great enough within 10 to 100 feet above the oil-water contact to attain S_{wi}. From the oil-water contact upward, S_w decreases gradually from 100% until it becomes equal to S_{wi}. In good quality reservoirs of substantial thickness, it is S_{wi} that must be estimated for assessment purposes.

Data from Prudhoe Bay Field (Fig. PP8) show that water saturation can vary considerably both laterally (areas in Fig. PP8) and vertically (zones in Fig. PP8) within a very large reservoir: values of S_w range from 7.5% to 58%. The variations in S_w in Prudhoe Bay Field reflect control by lithology, extent and dynamics of the hydrocarbon column, and fluid properties (Richardson and Holstein, 1994, Erickson and Sneider, 1997). In general, S_w declines in rocks with better reservoir quality, in locations where the greatest hydrocarbon column heights have been attained either at present or at some time during filling of the reservoir, and where buoyancy forces are the greatest due to the density difference between oil and water. In the

following discussion, we will ignore the latter two effects (height of hydrocarbon column and fluid properties) in order to establish a predictor of S_w based upon lithology and porosity.

In some oil fields, water content tends to a constant value above the oil-water transition zone (e.g., Buckles, 1965). In other words, porosity φ and irreducible water saturation S_{wi} may vary with depth, but the product φS_{wi} approximately equals a constant within a given formation. Support for the concept is mustered in Fig. PP9, where capillary pressure data at 300 psi, taken from Table PP4, is plotted on a plot of S_w versus φ, along with lines of constant φS_w. The grain size labels in Fig. PP9, taken from Asquith (1982), serve as a heuristic guide. The data conform to our expectations from grain size considerations: points from the coarse-grained Kekiktuk lie on a curve of low total water while points from the fine-grained Canning Formation lie in a regime of high total water. Data from the Endicott Field also support the concept (Fig. PP10): coarse grained units contain lower total water than fine grain units when data are averaged over an oil field.

Lacking a data-based methodology, we have adopted the φS_{wi} = constant concept, assigning a constant for each Play based upon lithology (Table PP7). For assessment purposes, a value of water saturation is derived for each value of the porosity distribution, using Table PP7. For example: if $\varphi_{50} = 0.15$ in the Turbidite Play, then $S_{wi50}=0.06/0.15 = 0.4$, or 40%. Water saturation values were limited to a maximum of 65% for cases where this simple rule produced values in excess of 65%.

VELOCITY AND DENSITY FROM WELL LOGS

Average values of velocity and density, useful for interpreting seismic records and gravity profiles, were obtained from well logs in Ellesmerian and basement rocks (Table PP8). The gamma ray was averaged over the same intervals; it is considered to be an indicator of shaliness. In most cases the entire formation was included in the average.

Similar estimates have been made by other workers. A comparison of the velocity data from Table PP8 with previous work is shown in Fig. PP11. A comparison of density data from Table PP8 with previous density estimates is shown in Fig. PP12 and in Fig. GR04.

ACKNOWLEDGEMENT

D. Houseknecht collected samples, arranged for the capillary pressure measurements, and provided the logarithmic plots of capillary pressure. J.E. Kibler assisted with data compilation and preparation of figures. Reviews by D. Hayba, R. Saltus, and K. Varnes led to improvements in the manuscript.

REFERENCES

Asquith, G., 1982, Basic well log analysis for geologists, American Association of Petroleum Geologists, Tulsa, OK, 216 p.

Buckles, R.S., 1965, Correlating and averaging connate water saturation data, J. Canadian Petroleum Technology, v. 4, n. 1, p. 42-52.

Dodge, W.S.Sr., J.L. Shafer, and R.E. Klimentidis, 1996, Capillary pressure: the key to producible porosity, Trans. of Society of Professional Well Log Analysts 37th Annual Logging Symposium, paper J.

Erickson, J.W. and R.M. Sneider, 1997, Structural and hydrocarbon histories of the Ivishak (Sadlerochit) reservoir, Prudhoe Bay Field, SPE Reservoir Engineering, v. 12, n. 1, p. 18-22.

Foland, R.L., and D.J. Lalla, 1987, Seismic-reflection data acquisition, processing, and interpretation, Chap. 17 *in* K.J. Bird and L.B. Magoon, eds., Petroleum geology of the northern part of the Arctic National Wildlife Refuge, Northeastern Alaska, U.S. Geological Survey Bulletin 1778, p. 235-243.

Jennings, J.B., 1987, Capillary pressure techniques: Application to exploration and development geology, American Association of Petroleum Geologists Bulletin, v. 71, n. 10., p. 1186-1209.

Johnsson, M.J., D.G. Howell, and K.J. Bird, 1993, Thermal maturity patterns in Alaska: implications for tectonic evolution and hydrocarbon potential, American Association of Petroleum Geologists Bulletin, v. 77, n. 11, p. 1874-1903.

Richardson, J.G., and E.D. Holstein, 1994, Comparison of water saturations from capillary pressure measurements with oil-base-mud core data, Ivishak (Sadlerochit) Reservoir, Prudhoe Bay Field, Society Petroleum Engineers No. 28593, 69th Annual Tech. Conf. p. 311-318.

Robbins, S.L., 1987, Gravity interpretation of the Coastal Plain, 1987, Chap. 15 *in* K.J. Bird and L.B. Magoon, eds., Petroleum geology of the northern part of the Arctic National Wildlife Refuge, Northeastern Alaska, U.S. Geological Survey Bulletin 1778, p. 219-224.

Schmoker, J.W. and T.C. Hester, 1990, Regional trends of sandstone porosity versus vitrinite reflectance--a preliminary framework, *in* V.F. Nuccio and C.E. Barker, eds., Applications of thermal maturity studies in energy exploration, Society Economic Paleontologists and Mineralogists, p. 53-60.

Woidneck, K., P. Behrman, C. Soule, and J. Wu, 1987, Reservoir description of the Endicott Field, North Slope, Alaska, *in* I. Tailleur and P. Weimer, eds., Alaskan North Slope Geology, Society Economic Paleontologists and Mineralogists, vol. 1, p. 41-59.

Table PP1. Thickness of reservoir-prone formations, from well log criteria. Net thickness is based upon a gamma-ray criterion. [The net/gross ratio for each formation in column 5 was computed as the average of the net-to-gross ratio for each well; hence numerical values differ from the ratio of average net thickness (column 4) to average gross thickness (column 3).]

Formation	Number of Wells	Average Gross Thickness (feet)	Average Net Thickness (feet)	Net/Gross Ratio
Sagavanirktok	11	2626	778	0.30
Staines Tongue of Sagavanirktok	6	1223	491	0.50
Mikkelsen Tongue of Canning	7	3095	380	0.14
Canning	10	2658	301	0.13
Thomson	6	205	172	0.87
Kemik	4	99	55	0.77
Sag River	2	63	58	0.93
Ledge	3	457	303	0.65
Lisburne	3	1860	--	--
Kekiktuk	2	756	167	0.22
Basement	4	680	246	0.42

Table PP2. Gross thickness in feet of Ellesmerian formations completely penetrated by wells. [Gross thickness values given here differ from those in Table PP1 because the number of wells differs.]

Formation	# Wells	Average Gross Thickness, Reservoir- prone (feet)	Average Gross Thickness, Non-reservoir (feet)	Sum Gross Ellesmerian (feet)	Formation Thickness/Total Thickness (ratio)	Reservoir Thickness/Total Thickness (ratio)
Kingak	9		1329		0.173	
Sag River	10	56			0.007	
Shublik	10		166		0.022	
Fire Creek	10		271		0.035	
Ledge	10	407			0.053	
Kavik	9		451		0.059	
Echooka	8		283		0.037	
Lisburne	5	2812			0.366	
Kayak	5		634		0.083	
Kekiktuk	4	1273			0.166	
Sum		4548	3134	7682	1.001	0.592

Table PP3. Permeability (millidarcy), porosity (%), and oil saturation (%) from laboratory analysis of samples from conventional cores, listed by well and by formation. Column labelled "M.Depth" gives measured depth of samples in feet. For index of short well names, see Table WL7. Average porosity (AvgPor), standard deviation (StdDev), and number of samples (#Samples) are given in first row for each formation.

Well	Formation	M.Depth	Perm.	Poro.	OilSat.	AvgPor	StdDev	#Samples
AkA1	MT Canning	12437		9.5		16.3	3.47	15
AkA1	MT Canning	12444		19.3				
AkA1	MT Canning	12468		14.3				
AkA1	MT Canning	12474		17.9				
AkA1	MT Canning	12476		14.3				
AkA1	MT Canning	12528		12.7				
AkA1	MT Canning	12535		16.5				
AkA1	MT Canning	12566		15.9				
AkA1	MT Canning	12574		23.1				
AkA1	MT Canning	12579		19.3				
AkA1	MT Canning	12605		10.3				
AkA1	MT Canning	12613		17.7				
AkA1	MT Canning	12614		17.9				
AkA1	MT Canning	12615		17.1				
AkA1	MT Canning	12640		18.7				
AkC1	Thomson	13562		16.6		17.64	1.87	5
AkC1	Thomson	13564		16.1				
AkC1	Thomson	13566		19.9				
AkC1	Thomson	13570		15.7				
AkC1	Thomson	13572		19.9				
AkF1	MT Canning	12063		15.9		19.03	2.85	16
AkF1	MT Canning	12072	4.43	19.6				
AkF1	MT Canning	12074	1.5	17.1				
AkF1	MT Canning	12075		20.0				
AkF1	MT Canning	12076		21.1				
AkF1	MT Canning	12576		22.8				
AkF1	MT Canning	12584		11.6				
AkF1	MT Canning	12599		22.0				
AkF1	MT Canning	12600		18.8				
AkF1	MT Canning	12601	11.3	21.9				
AkF1	MT Canning	12602		22.8				
AkF1	MT Canning	12603		18.2				
AkF1	MT Canning	12906		16.0				
AkF1	MT Canning	12907		19.3				
AkF1	MT Canning	12908		18.4				
AkF1	MT Canning	12909		18.9				

Table PP3 cont.

Well	Formation	M.Depth	Perm.	Poro.	OilSat.	AvgPor	StdDev	#Samples
Alp	ST Sagav	8134.5	258	21.3	0	18.46	4.79	24
Alp	ST Sagav	8135	207	18.3	0			
Alp	ST Sagav	8135.5	3350	23.5	0			
Alp	ST Sagav	8136	4220	22.8	0			
Alp	ST Sagav	8136.5	1320	24.0	0			
Alp	ST Sagav	8137	385	26.8	0			
Alp	ST Sagav	8137.5	630	21.7	0			
Alp	ST Sagav	8138	324	21.8	0			
Alp	ST Sagav	8138.5	0.8	12.3	0			
Alp	ST Sagav	8139.5	0.3	10.4	0			
Alp	ST Sagav	8140.5	0.4	8.8	0			
Alp	ST Sagav	8141.5	53	19.4	0			
Alp	ST Sagav	8142	217	22.5	0			
Alp	ST Sagav	8142.5	375	24.9	0			
Alp	ST Sagav	8143	156	24.4	0			
Alp	ST Sagav	8143.5	13	15.5	0			
Alp	ST Sagav	8144.5	8.1	16.1	0			
Alp	ST Sagav	8145.5	2.9	14.2	0			
Alp	ST Sagav	8147.5	5.6	16.6	0			
Alp	ST Sagav	8148.5	2.2	15.2	0			
Alp	ST Sagav	8149.5	1.1	16.8	0			
Alp	ST Sagav	8150.5	3.1	14.2	0			
Alp	ST Sagav	8154.5	1.7	17.3	0			
Alp	ST Sagav	8162.5	1.3	14.3	0			
Auro	Canning	9632	0.1	8	0	7.35	0.65	6
Auro	Canning	9635	0.2	8	0			
Auro	Canning	9646.5	1.6	6.4	0			
Auro	Canning	9647	0.2	6.6	0			
Auro	Canning	9654.5	0.2	7.3	0			
Auro	Canning	9668.5	3.7	7.8	0			
Bad1	PbblSh	12560.5	0.1	3.2	2.3	4.25	0.83	4
Bad1	PbblSh	12562.5	0.1	3.8	15.7			
Bad1	PbblSh	12563	0.1	4.6	3.1			
Bad1	PbblSh	12564.5	0.1	5.4	15.7			
Bad1	Kemik	12606.5	0.1	2	35.7	3.35	1.21	28
Bad1	Kemik	12609.5	0.1	3.5	28.5			
Bad1	Kemik	12611	0.1	3	28			
Bad1	Kemik	12611.5	0.1	2.9	26.2			
Bad1	Kemik	12612	0.1	2.2	46.3			
Bad1	Kemik	12614.5	0.1	2.2	26.1			
Bad1	Kemik	12615.5	0.1	2.6	23.9			
Bad1	Kemik	12617.5	0.1	4.1	42.1			
Bad1	Kemik	12618.5	0.1	3.1	2.3			

Click here or on this symbol in the toolbar to return.

Table PP3 cont.

Well	Formation	M.Depth	Perm.	Poro.	OilSat.	AvgPor	StdDev	#Samples
Bad1	Kemik	12619.5	0.1	3.6	4			
Bad1	Kemik	12620	0.8	3.9	16.3			
Bad1	Kemik	12621.5	0.1	3.4	14.3			
Bad1	Kemik	12623	0.1	3.8	36.2			
Bad1	Kemik	12624	0.1	7.1	8.7			
Bad1	Kemik	12624.5	0.1	2.6	13.3			
Bad1	Kemik	12625.5	0.1	3.1	20.1			
Bad1	Kemik	12627	0.1	3.5	26			
Bad1	Kemik	12627.5	0.1	7	22			
Bad1	Kemik	12628.5	0.1	3.1	29.7			
Bad1	Kemik	12630.5	0.1	3.1	33.6			
Bad1	Kemik	12631.5	0.1	3.9	18.1			
Bad1	Kemik	12632	0.1	3.9	45.7			
Bad1	Kemik	12634.5	0.1	3.6	11.8			
Bad1	Kemik	12635	0.1	3.1	18.3			
Bad1	Kemik	12636.5	0.1	1.6	9.1			
Bad1	Kemik	12637.5	0.1	2.8	22.8			
Bad1	Kemik	12641.5	2.9	3.4	6.2			
Bad1	Kemik	12642.5	0.1	1.8	5.4			
Bad1	Kayak	12647.5	0.1	1.7	4.4	2.57	1.22	15
Bad1	Kayak	12649.5	0.1	1.6	6			
Bad1	Kayak	12654.5	0.1	1.2	6			
Bad1	Kayak	12665.5	0.1	1.3	5.4			
Bad1	Kayak	12675	0.2	2.9	4.8			
Bad1	Kayak	12679.5	0.1	3	2.4			
Bad1	Kayak	12682	0.1	3.6	5.9			
Bad1	Kayak	12682.5	0.4	3.8	1.8			
Bad1	Kayak	12683.5	0.1	3.6	2			
Bad1	Kayak	12685	0.1	3.1	20.5			
Bad1	Kayak	12686	0.1	3.3	10.8			
Bad1	Kayak	12686.5	0.1	1.2	0			
Bad1	Kayak	12687.5	0.1	1.4	9.9			
Bad1	Kayak	12688.5	0.1	5.4	5.6			
Bad1	Kayak	12689	2.8	1.5	4.8			
Bad1	Kekiktuk	12690.5	0.7	3.4	2.1	4.71	2.12	15
Bad1	Kekiktuk	12691	0.1	3.9	1.8			
Bad1	Kekiktuk	12692.5	0.1	4.1	0			
Bad1	Kekiktuk	12693.5	3.6	7.3	0			
Bad1	Kekiktuk	12694.5	1.4	9	0			
Bad1	Kekiktuk	12696	1	5.6	0			
Bad1	Kekiktuk	12696.5	0.1	3.4	0			
Bad1	Kekiktuk	12697	0.1	1.6	0			
Bad1	Kekiktuk	12698	0.1	3	22.8			
Bad1	Kekiktuk	12698.5	0.1	4.8	3			
Bad1	Kekiktuk	12699	0.1	3.6	11.8			

Click here or on this symbol in the toolbar to return.

Table PP3 cont.

Well	Formation	M.Depth	Perm.	Poro.	OilSat.	AvgPor	StdDev	#Samples
Bad1	Kekiktuk	12701.5	0.1	2.9	10.1			
Bad1	Kekiktuk	12702.5	0.1	6.1	1.1			
Bad1	Kekiktuk	12703	0.1	8.7	27.3			
Bad1	Kekiktuk	12703.5	0.1	3.2	20.1			
Bad1	Kekiktuk	12824.5	8.3	24.9	7.3	17.26	5.79	27
Bad1	Kekiktuk	12825.5	12	26.7	3.3			
Bad1	Kekiktuk	12826.5	0.1	13.3	2.3			
Bad1	Kekiktuk	12827.5	9.2	26.3	0.3			
Bad1	Kekiktuk	12828.5	9.7	27.1	11.4			
Bad1	Kekiktuk	12829.5	2.5	21.3	8.1			
Bad1	Kekiktuk	12830	3.8	18.3	5.1			
Bad1	Kekiktuk	12831.5	1.2	18.7	10.3			
Bad1	Kekiktuk	12832.5	1	20.1	12.2			
Bad1	Kekiktuk	12833	0.7	18.9	18.2			
Bad1	Kekiktuk	12834	0.8	14.4	17.4			
Bad1	Kekiktuk	12836	2.7	19.5	9.1			
Bad1	Kekiktuk	12836.5	2	16.9	7.2			
Bad1	Kekiktuk	12838	4.5	23.9	5.9			
Bad1	Kekiktuk	12838.5	0.1	6.1	18.8			
Bad1	Kekiktuk	12840	0.1	12.5	15.1			
Bad1	Kekiktuk	12841	2.8	22.2	6.7			
Bad1	Kekiktuk	12841.5	1	19	13.1			
Bad1	Kekiktuk	12842.5	1.4	19	4.1			
Bad1	Kekiktuk	12843.5	0.6	15.9	10.6			
Bad1	Kekiktuk	12844.5	1	6.7	26.3			
Bad1	Kekiktuk	12845.5	0.1	8.9	9.3			
Bad1	Kekiktuk	12846.5	0.1	9.2	17.1			
Bad1	Kekiktuk	12848	0.1	12	15.8			
Bad1	Kekiktuk	12848.5	0.1	13.8	5.6			
Bad1	Kekiktuk	12849	0.1	14.7	4.4			
Bad1	Kekiktuk	12850	0.1	15.6	3.6			
Bad1	Kekiktuk	12851.5	0.1	2.2	25.4	2.02	0.81	10
Bad1	Kekiktuk	12852.5	0.1	1.6	17.6			
Bad1	Kekiktuk	12853.5	0.2	3	2.3			
Bad1	Kekiktuk	12854.5	0.1	2.9	2.5			
Bad1	Kekiktuk	12856	3.2	3.3	2.1			
Bad1	Kekiktuk	12860	0.1	1.7	0			
Bad1	Kekiktuk	12867.5	0.1	0.7	0			
Bad1	Kekiktuk	12875	0.1	1	0			
Bad1	Kekiktuk	12881.5	0.5	2.1	0			
Bad1	Kekiktuk	12883	0.1	1.7	0			
Bad2	Canning	10736.5		18.9	56.4			
CRA1	Sag River	4289	0.1	4.4	0	4.18	0.81	5
CRA1	Sag River	4289.5	0.1	4.8	0			

Click here or on this symbol in the toolbar to return.

Table PP3 cont.

Well	Formation	M.Depth	Perm.	Poro.	OilSat.	AvgPor	StdDev	#Samples
CRA1	Sag River	4290	0.1	5.2	0			
CRA1	Sag River	4291.5	0.1	3.1	0			
CRA1	Sag River	4292	0.1	3.4	0			
CRA1	Ledge	4868.5	0.1	1.1		2.34	1.32	47
CRA1	Ledge	4870	0.1	0.8				
CRA1	Ledge	4870.5	0.1	0.8				
CRA1	Ledge	4871.5	0.1	0.6				
CRA1	Ledge	4872.5	0.1	0.9				
CRA1	Ledge	4873.5	0.1	1.4				
CRA1	Ledge	4874.5	0.1	0.9				
CRA1	Ledge	4875.5	0.1	1.3				
CRA1	Ledge	4876.5	0.1	2.2				
CRA1	Ledge	4879	0.1	2.1	0			
CRA1	Ledge	4880.5	0.1	3	0			
CRA1	Ledge	4881.5	0.1	5	0			
CRA1	Ledge	4882.5	0.1	4.5	0			
CRA1	Ledge	4883.5	0.1	5.5	0			
CRA1	Ledge	4884.5	0.1	6.1	0			
CRA1	Ledge	4885.5	0.1	3.8	0			
CRA1	Ledge	4886.5	0.1	1.7	0			
CRA1	Ledge	4887.5	0.1	1.8	0			
CRA1	Ledge	4888.5	0.1	2.9	0			
CRA1	Ledge	4889.5	0.1	3.3	0			
CRA1	Ledge	4890.5	0.1	3.3	0			
CRA1	Ledge	4891.5	0.1	1.6	0			
CRA1	Ledge	4892.5	0.1	3.1	0			
CRA1	Ledge	4893.5	0.1	3.9	0			
CRA1	Ledge	4894.5	0.1	4.3	0			
CRA1	Ledge	4895.5	0.1	3.4	0			
CRA1	Ledge	4896.5	0.1	3.8	0			
CRA1	Ledge	4897.5	0.1	3	0			
CRA1	Ledge	4898.5	0.1	2.4	0			
CRA1	Ledge	4899	0.1	3	0			
CRA1	Ledge	4900.5	0.1	3.1	0			
CRA1	Ledge	4901	0.1	2.4	0			
CRA1	Ledge	4902	0.1	1.4	0			
CRA1	Ledge	4903.5	0.1	1.8	0			
CRA1	Ledge	4904.5	0.1	2.1	0			
CRA1	Ledge	4905.5	0.1	1.4	0			
CRA1	Ledge	4906.5	0.1	1.4	0			
CRA1	Ledge	4907.5	0.1	1.1	0			
CRA1	Ledge	4908.5	0.1	1.3	0			
CRA1	Ledge	4909.5	0.1	1.3	0			
CRA1	Ledge	4910.5	0.1	1.2	0			
CRA1	Ledge	4911.5	0.1	1.5	0			

Table PP3 cont.

Well	Formation	M.Depth	Perm.	Poro.	OilSat.	AvgPor	StdDev	#Samples
CRA1	Ledge	4912.5	0.1	1.3	0			
CRA1	Ledge	4913.5	0.1	1.2	0			
CRA1	Ledge	4914.5	0.1	1.7	0			
CRA1	Ledge	4985.5	0.1	1.4	0			
CRA1	Ledge	4986.5	0.1	2.8	0			
CRB1	Ledge	8955	0	3.4	0	2.57	1.83	18
CRB1	Ledge	8956	0.4	5.9	0			
CRB1	Ledge	8957	0.3	8.2	0			
CRB1	Ledge	8958	0.1	1.4	0			
CRB1	Ledge	8959	0	1.5	0			
CRB1	Ledge	8960	0.1	2.9	0			
CRB1	Ledge	8961	3.6	2.4	0			
CRB1	Ledge	8962	1.1	2.6	0			
CRB1	Ledge	8963	0.1	2.9	0			
CRB1	Ledge	8964	0.4	2.3	0			
CRB1	Ledge	8965	0.1	2.1	0			
CRB1	Ledge	8966	0	0.7	0			
CRB1	Ledge	8967	0.1	1.3	0			
CRB1	Ledge	8968	0.3	1.5	0			
CRB1	Ledge	8969		2.3	0			
CRB1	Ledge	8970	0	1	0			
CRB1	Ledge	8971	0	0.5	0			
CRB1	Ledge	8972	0	3.3	0			
Gyr	Sagav	5463.5	38	13.3	1	10.25	2.85	31
Gyr	Sagav	5464.5	0.8	9	3			
Gyr	Sagav	5465.5	2.1	9.7	2.1			
Gyr	Sagav	5466.5	7.1	11.7	8.7			
Gyr	Sagav	5467.5	4.9	11.4	4.7			
Gyr	Sagav	5468.5	22	12.4	2.2			
Gyr	Sagav	5469.5	35	12.2	2.2			
Gyr	Sagav	5470.5	21	12.7	4.2			
Gyr	Sagav	5471	48	12.4	1.1			
Gyr	Sagav	5472.5	71	14.1	2.3			
Gyr	Sagav	5473.5	18	11.7	1.2			
Gyr	Sagav	5474.5	3.4	9.4	1.4			
Gyr	Sagav	5475.5	78	13	1.1			
Gyr	Sagav	5476.5	0.4	4.5	0			
Gyr	Sagav	5477.5	0.3	3.2	0			
Gyr	Sagav	5478.5	0.2	4.5	3			
Gyr	Sagav	5479.5	0.1	4.7	0			
Gyr	Sagav	5480	0.1	4.9	0			
Gyr	Sagav	5481.5	0.1	9.8	0			
Gyr	Sagav	5482.5	0.2	10.2	1.3			

Click here or on this symbol in the toolbar to return.

Table PP3 cont.

Well	Formation	M.Depth	Perm.	Poro.	OilSat.	AvgPor	StdDev	#Samples
Gyr	Sagav	5483.5	1	10.8	2.4			
Gyr	Sagav	5484.5	1.6	11.6	1.2			
Gyr	Sagav	5485	1.6	11.4	4.8			
Gyr	Sagav	5486.5	0.8	11.5	2.4			
Gyr	Sagav	5487.5	1.2	11.9	4.5			
Gyr	Sagav	5488.5	1.1	11.7	1.1			
Gyr	Sagav	5489.5	1	11.6	4.6			
Gyr	Sagav	5490.5	0.9	11.7	1.7			
Gyr	Sagav	5491.5	1	11.6	1.2			
Gyr	Sagav	5492.5	0.2	10.3	6			
Gyr	Sagav	5493	0.1	8.9	0			
Kav2	Ledge	6220	0.01	1.4		3.3	1.40	6
Kav2	Ledge	6230	0.01	2.8				
Kav2	Ledge	6231	0.01	5.9				
Kav2	Ledge	6232	0.01	3.4				
Kav2	Ledge	6235	0.01	2.4				
Kav2	Ledge	6241	0.02	3.9				
Kav3	Ledge	5321	0.02	6.3		4.77	1.70	6
Kav3	Ledge	5325	0.01	3.9				
Kav3	Ledge	5424	0.04	7.6				
Kav3	Ledge	5429	0.01	3.1				
Kav3	Ledge	5437	0.01	4.8				
Kav3	Ledge	5439	0.01	2.9				
PtT1	Thomson	12837		11.7		15.04	2.67	10
PtT1	Thomson	12838		12.6				
PtT1	Thomson	12858		15.9				
PtT1	Thomson	12869		16.5				
PtT1	Thomson	12875		13.1				
PtT1	Thomson	12876		14				
PtT1	Thomson	12913		15.6				
PtT1	Thomson	12922		14.9				
PtT1	Thomson	12932		14.3				
PtT1	Thomson	12995		21.8				
PtT2	Canning	9875		10.6		16.25	3.34	14
PtT2	Canning	9880		11.3				
PtT2	Canning	10156		13.2				
PtT2	Canning	10157		21.6				
PtT2	Canning	10196		14.5				
PtT2	Canning	11595		17.7				
PtT2	Canning	11597		14.8				
PtT2	Canning	11607		13.9				
PtT2	Canning	11619		18.7				

Table PP3 cont.

Well	Formation	M.Depth	Perm.	Poro.	OilSat.	AvgPor	StdDev	#Samples
PtT2	Canning	11634		15.3				
PtT2	Canning	11636		16.9				
PtT2	Canning	11775		21.3				
PtT2	Canning	11777		20.1				
PtT2	Canning	11778		17.6				
PtT3	Thomson	13673		16.4		22.53	3.79	8
PtT3	Thomson	13676		16.3				
PtT3	Thomson	13689		24				
PtT3	Thomson	13766		23.9				
PtT3	Thomson	13768		25.9				
PtT3	Thomson	13777		25				
PtT3	Thomson	13780		26.6				
PtT3	Thomson	13788		22.1				
Mikk	Kemik	11690	0.0006	4.2		8.88	3.45	10
Mikk	Kemik	11699	0.0109	7.8				
Mikk	Kemik	11702	0.0012	6.2				
Mikk	Kemik	11703	0.0096	8.1				
Mikk	Kemik	11704	0.0384	9.3				
Mikk	Kemik	11730		9.5				
Mikk	Kemik	11733		14.7				
Mikk	Kemik	11734		12.2				
Mikk	Kemik	11735		13				
Mikk	Kemik	11736		3.8				
WSt1	MTCanning	7711		10.2		10.83	1.65	3
WSt1	MTCanning	7756		13.1				
WSt1	MTCanning	7768	0.0013	9.2				
WSt1	Canning	10583		12.8		11.93	2.53	13
WSt1	Canning	10589		4.9				
WSt1	Canning	10590		12.7				
WSt1	Canning	10591	1.03	15.4				
WSt1	Canning	10592		13.5				
WSt1	Canning	10594		10.3				
WSt1	Canning	10597		13.3				
WSt1	Canning	11695		11.3				
WSt1	Canning	11696	1.68	13.5				
WSt1	Canning	11709.5	1.81	12.4				
WSt1	Canning	11710		10.8				
WSt1	Canning	11711		13.3				
WSt1	Canning	11712.5		10.9				
WSt1	PbblSh	13068	0.001	6.6		7.08	0.34	4
WSt1	PbblSh	13112	0.001	7.2				
WSt1	PbblSh	13113		7.4				
WSt1	PbblSh	13114		7.1				

Table PP4. Porosity and permeability by conventional measurements on plugs cut from core, and by mercury-injection-capillary-pressure (MICP). Surface samples include a "DH" designation. Samples from wells: G, Gyr; WM2, West Mikkelsen 2; WM1, West Mikkelsen 1; K2, Kemik 2. Irreducible water saturation at 300 psi is listed in column 7 for samples from wells. An average appears in column 8 for the plug porosity data from wells.

Formation	Sample	Plug Porosity (%)	Plug Perm (md)	MICP Porosity (%)	MICP Perm (md)	Swi @ 300 psi	Average Plug Porosity (%)
Sagavanirktok	95DH-21	16.2	281	15.5	275		
	95DH-22	17.1	473	17.7	376		
	96DH-120			35.7	81		
	96DH-122	7.6	2.5	3.06	0.027		
	96DH-153	26.4	1150	25.2	517		
	96DH-154	13.0	39	12.8	44.8		
	97DH-21	6.5	0.05	4.8	0.03		
	97DH-23	8.6	0.66	8.3	0.12		
	97DH-25	15.6	86	14.4	54.5		
	97DH-32	7.7	0.05	7.3	0.05		
	97DH-38	13.9	18	13.6	33.0		
	97DH-42	10.4	16	9.7	8.1		
	97DH-70	16.9	4.69	16.6	6.2		
	97DH-71	19.2	10	18.1	10.0		
	97DH-73	6.6	0.08	6.4	0.09		
	97DH-82	16.1	46	15.8	41.5		
	97DH-85	23	122	22	82.0		
	97DH-88	19	165	18.1	138		
	97DH-90	34.5	11850	32.6	3973		
	97DH-95	24.7	4110	23.3	2026		
	97DH-100	24.9	6360	23.6	2575		
	97DH-101	11.1	0.55	11.7	0.64		
	G-5463	14.4	43	13.8	45.3	0.20	11.70
	G-5469	14.3	79	13.4	70.6	0.18	
	G-5475	15.3	64	13.2	50.9	0.18	
	G-5480	3.9	4.4	3.47	0.28	0.59	
	G-5482	12.9	0.66	9.96	0.55	0.50	
	G-5489	10.6	0.83	11	0.93	0.47	
	G-5491	10.5	0.72	11.8	0.75	0.51	
Canning	95DH-1	5.4	0.03	3.99	0.003		
	95DH-4c	5.6	0.08	5.78	0.053		
	95DH-44	7.7	0.17	5.5	0.087		
	96DH-75	3.9	0.02	4.16	0.006		
	96DH-119	8.5	0.009	6.27	0.023		
	96DH-121	2.4	0.002	1.21	0.001		
	97DH-5	11.8	0.90	10.9	0.82		
	97DH-9	8.2	0.10	8.1	0.13		

Click here or on this symbol in the toolbar to return.

Table PP4 cont.

Formation	Sample	Plug Porosity (%)	Plug Perm (md)	MICP Porosity (%)	MICP Perm (md)	Swi @ 300 psi	Average Plug Porosity (%)
	97DH-12	4.0	12.	3.3	0.002		
	97DH-15	5.3	0.20	4.2	0.02		
	WM2-10416	5.7	0.03	5.33	0.0001		11.92
	WM2-10425	20.8	16	18.5	10	0.33	
	WM2-10429	5.5	0.029	4.96	0.0001		
	WM2-10497	14.8	1.4	11.3	0.27	0.65	
	WM2-10506	19.1	26	18.6	13.4	0.32	
	WM2-10553	5.6		5.1	0.0001		
Sabbath Creek	96DH-106	4.2	0.24	3.37	0.008		
	96DH-108	2.6	1	2.01	0.003		
	96DH-110	5.7	0.49	5.11	0.084		
	96DH-113	7.8		6.55	0.28		
	96DH-114	7.0	0.68	5.62	0.108		
	96DH-118	9.1	1.4	8.4	0.37		
Kemik	96DH-15	2.0	0.004	1.57	0.001		
	96DH-68	3.3	0.02	3.34	0.005		
Thomson	WM1-11239	4.4	0.07	4.32	0.014		3.52
	WM1-11264	5.5	0.12	5.85	0.05		
	WM1-11285	2.6	0.009	1.55	0.0001		
	WM1-11300	1.0	0.01	1.11	0.0001		
	WM1-11304	4.1	0.058	4.1	0.016		
Shublik	96DH-21	30.5	355	30	102		
Ivishak	95DH-51	7.9	0.03	6.61	0.012		
	96DH-9	1.3	0.011	0.78	0.001		
	96DH-123	8.2	0.36	7.88	0.025		
	K2-6219	1.4	0.01				3.30
	K2-6229	2.8	0.01				
	K2-6230	5.9	0.01				
	K2-6231	3.4	0.01				
	K2-6234	2.4	0.01				
	K2-6240	3.9	0.02				
	K3-5320	6.3	0.02				4.77
	K3-5324	3.9	0.01				
	K3-5423	7.6	0.04				
	K3-5429	3.1	0.01				
	K3-5436	4.8	0.01				
	K3-5438	2.9	0.01				
Lisburne	WM1-11305	1.1		0.81	0.0001		12.47

Click here or on this symbol in the toolbar to return.

Table PP4 cont.

Formation	Sample	Plug Porosity (%)	Plug Perm (md)	MICP Porosity (%)	MICP Perm (md)	Swi @ 300 psi	Average Plug Porosity (%)
	WM1-11350	26.9	107	22.4	90.2	0.06	
	WM1-11374	7.7	0.02	8.13	0.005		
	WM1-11392	23.4	2.3	20.4	2.52	0.31	
	WM1-11402	0.9		0.27	0.0001		
	WM1-11706	18.7		17.8	15.3	0.18	
	WM1-11717	8.6	0.058	8.96	0.031		
Kekiktuk	WM1-13728	11.6	38	11.6	40.5	0.06	10.53
	WM1-14049	9.1	9.2	8.48	7.54	0.12	
	WM1-14183	10.9	15	10.2	12.8	0.16	

Table PP5. Grain density averages (g/cm^3), listed by formation and by well, based upon grain density measurements obtained from conventional cores. Coal samples, recognized by their low density values, were excluded from the averages. A weighted average for each formation (except the Kekiktuk) appears in column 5. The Kekiktuk data were not averaged because of the presence of pyrite in some samples in the interval with 18 samples. Individual grain density data are available in digital files. [MTCanning: Mikkelsen Tongue of Canning Formation; STSagavanirktok: Staines Tongue of Sagavanirktok Formation.]

Formation	Well	Grain density average in a well (g/cm^3)	Number of points in a well	Grain density, average for formation (g/cm^3)
Sagavanirktok	Gyr 1	2.65	31	2.65
MTCanning	Alaska State A-1	2.7	15	2.67
MTCanning	Alaska State F-1	2.618	5	
MTCanning	Alaska State F-1	2.64	7	
MTCanning	Alaska State F-1	2.683	4	
MTCanning	W Staines 18-9-23	2.683	3	
STSagavanirktok	Alpenglow State 1	2.667	24	2.65
STSagavanirktok	Badami 1	2.622	13	
Canning	Badami 1	2.611	26	2.64
Canning	Badami 2	2.65	1	
Canning	Point Thomson 2	2.76	2	
Canning	Point Thomson 2	2.76	3	
Canning	Point Thomson 2	2.742	9	
Canning	W Staines 18-9-23	2.611	7	
Canning	W Staines 18-9-23	2.585	6	
Canning	Aurora 1	2.728	6	2.73
Hue/Gamma	Badami 1	2.63	4	2.63
Pebble Shale	W Staines 18-9-23	2.74	4	2.74
Kemik	Badami 1	2.72	28	2.71
Kemik	Mikkelsen Bay 1	2.699	10	
Thomson	Alaska State C-1	2.962	5	2.86
Thomson	Point Thomson 1	2.814	10	
Thomson	Point Thomson 3	2.84	8	
Ledge	Kavik Unit 2	2.67	6	2.67
Ledge	Kavik Unit 3	2.675	2	
Ledge	Kavik Unit 3	2.67	4	
Kayak	Badami 1	2.61	15	2.61
Kekiktuk	Badami 1	2.63	10	
Kekiktuk	Badami 1	2.635	29	
Kekiktuk	Badami 1	2.71	18	Pyrite in some samples

Table PP6. Coefficients for prediction of porosity φ from vitrinite reflectance R_o, $\varphi_j = A_j R_o^{Bj}$, where j = 100, 95, 75, 50, 25, 5, 0. Expression from Schmoker and Hester (1990), with coefficients added for the 100, 95, 5, and 0 percentiles.							
Percent greater than	100	95	75	50	25	5	0
A coefficient	1.9	3.2	5.8	7.4	10.0	14.0	19.0
B coefficient	-1.55	-1.39	-1.15	-1.04	-0.89	-0.78	-0.70

Table PP7. Values of φS_{wi} = constant assigned to each play in this study for computation of S_{wi} from φ distribution.		
Play	Predominant Formation in Play	$\varphi S_{wi} \mid_{constant}$
Topset	Sagavanirktok	0.05
Turbidite	Canning	0.06
Wedge	Canning	0.04
Thomson	Thomson	0.06
Kemik	Kemik	0.06
Undeformed Franklinian	Basement carbonates	0.02
Thin-skinned Thrust Belt	Canning	0.06
Deformed Franklinian	Ellesmerian	0.02
Ellesmerian	Sadlerochit and Lisburne	0.035
Niguanak-Aurora	Basement	0.025

Table PP8. Velocity, density, and gamma ray averages from well logs in Ellesmerian and basement rocks. Depths and thicknesses are measured depths, in feet. Velocities are in feet per second, densities are in grams/cc, gamma ray in API units. Values are averages between formation boundaries except for the two basement carbonate samples. An asterisk (*) indicates that rough hole intervals were excluded from averages.

Formation	Well	Top Depth	Bottom Depth	Thickness	Velocity Average	Velocity Std. Dev.	Density Average	Density Std. Dev.	Gamma Ray Average	Lithology
Katakturuk Dolomite	Canning River A-1	8240	8874	634	20853	877	2.80	0.05	6	
Basement carbonate	Alaska State D-1	12735	12880	145	20571	810	2.71		26	Selected interval of carbonates.
Basement carbonate	Alaska State A-1	13265	13400	135	19497	1147	2.72		18	Selected interval of carbonates.
Basement rocks	E. Mikkelsen*	13550	15190	1421	17900	1493	2.64		82	Interbedded shale, carbonaceous shale, and limestone.
Basement rocks	Alaska State F-1	13920	14290	370	16288	1187	2.72	0.09	106	Interbedded shale, dolomite, and sandstone.
Basement rocks	Point Thomson 2	13115	14105	990	16084	1786	2.76	0.05	85	Interbedded phyllite and carbonate
Basement rocks	Point Thomson 3	13935	14130	195	15819	536	2.67	0.04	136	Predominantly phyllite.
Basement rocks	W. Mikkelsen 2	11630	11910	280	17003	1020	2.72	0.03	151	Shale with quartzite and argillite
Kekiktuk & Kayak (Endicott)	Mikkelsen Bay State 1	13800	16574	2774	13884	2441	2.52	0.26	75	Shale; mixed lithology of sandstone, coal, siltstone, and shale.
Kekiktuk & Kayak (Endicott)	Kavik 1	8778	9535	757	13469	2098	2.42	0.20	72	Shale; mixed lithology of siltstone, sandstone, shale.
Kekiktuk & Kayak (Endicott)	E. Mikkelsen Bay State 1	12345	13529	1184	12224	1512			119	Shale; mixed lithology of shale, sandstone, coal, siltstone
Kekiktuk & Kayak (Endicott)	West Mikkelsen State 1	12792	15581	2789	14150	2449	2.19	0.21	88	Shale; mixed lithology of sandstone, siltstone, shale.
Lisburne*	Beli Unit 1	12422	14600	2178	19541	997	2.69		27	Limestone and dolomite
Lisburne	Kavik 1	5555	8778	3223	15674	773	2.70	0.11	24	Dolomite and limestone
Lisburne	Canning River A-1	5675	7980	2305	19733	1373	2.74	0.07	32	Dolomite and limestone
Sadlerochit & Shublik	Beli Unit 1	11145	12422	1277	14697	1251	2.40	0.20	62	Sandstone, siltstone, shale, and limestone
Sadlerochit & Shublik	Kavik 1	4230	5555	1325	11877	2293	2.59	0.11		Sandstone, siltstone, shale, and limestone
Sadlerochit & Shublik	Canning River A-1	4275	5675	1400	15100	1816	2.64	0.09	78	Sandstone, siltstone, shale, and limestone
Kingak	Kemik Unit 1	4730	8476	3746	9378	1199			76	Shale
Kingak, Kupurak, Pebble shale	Aurora 1	15930	17740	1810	13011	1708	2.61	0.08	70	shale; sandstone; shale; overpressured
Kingak, Kemik, Pebble shale	West Kavik 1	12364	13190	826	10704	993			79	shale; sandstone; shale
Kingak, Kemik, Pebble shale	Canning River A-1	3110	4275	1165	10586	1197	2.42	0.13	90	shale; sandstone; shale

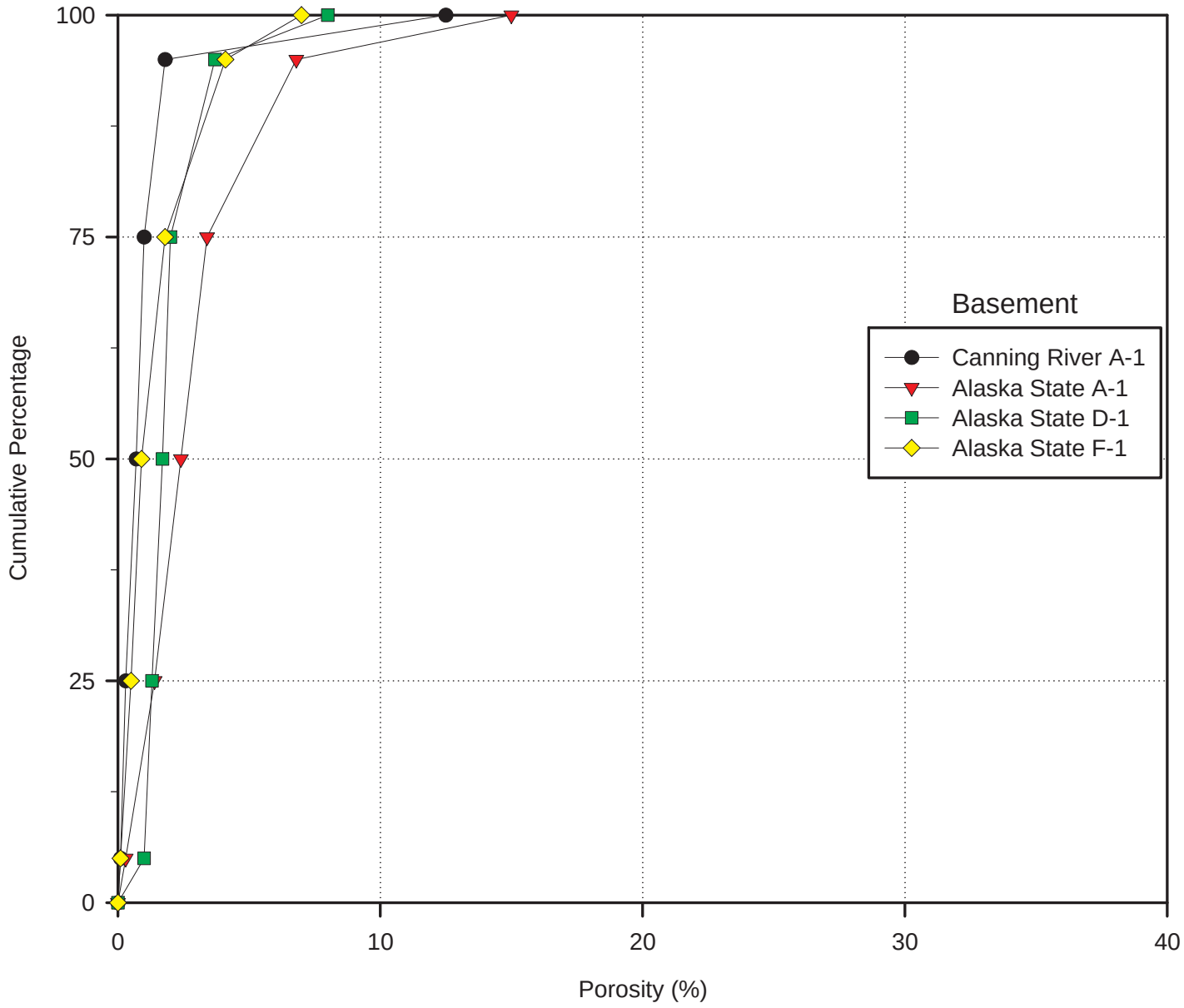

Figure PP1a. Cumulative distributions of porosity from well logs for basement carbonates.

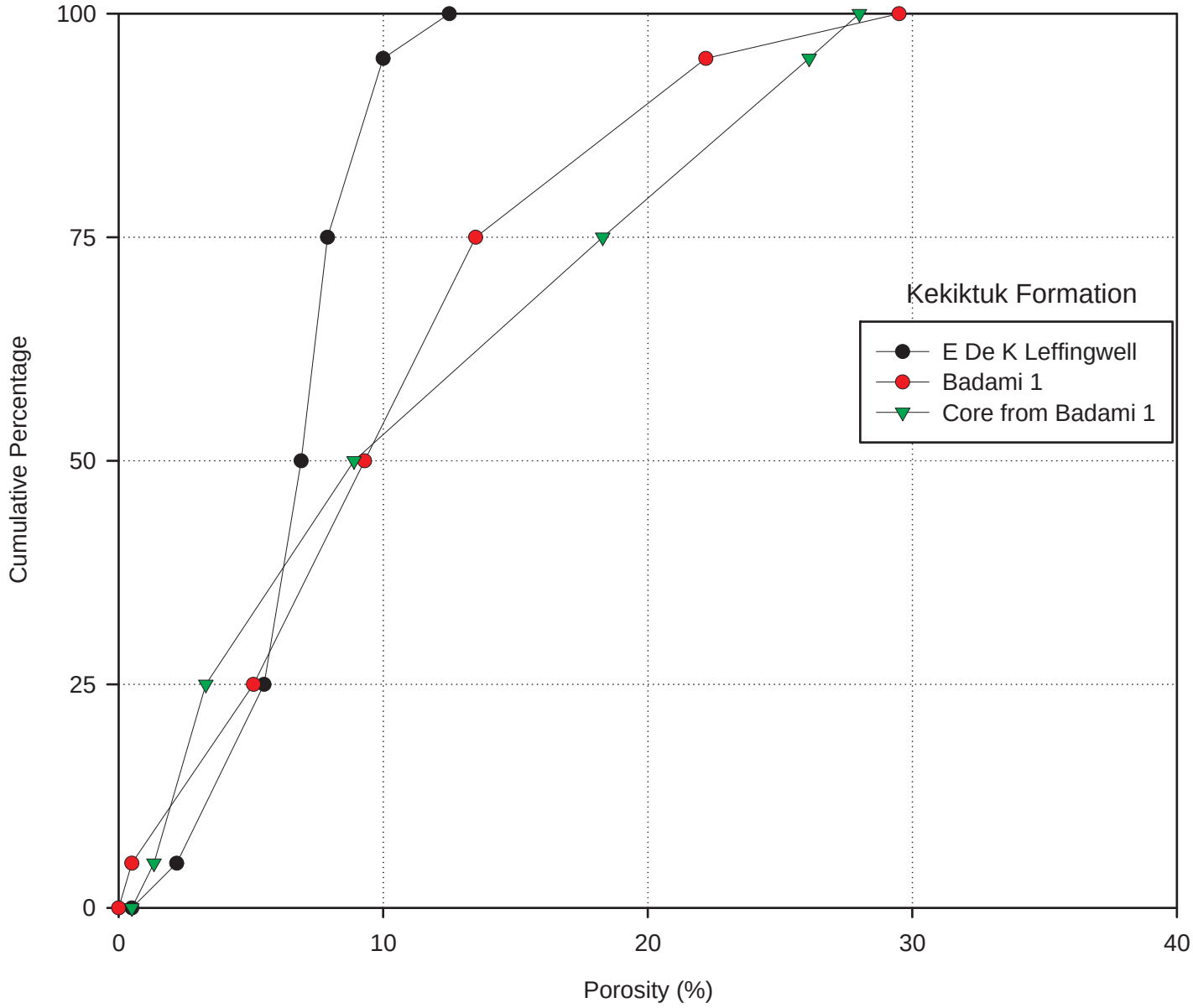

Figure PP1b. Cumulative distributions of porosity from well logs and core samples for Kekiktuk Formation.

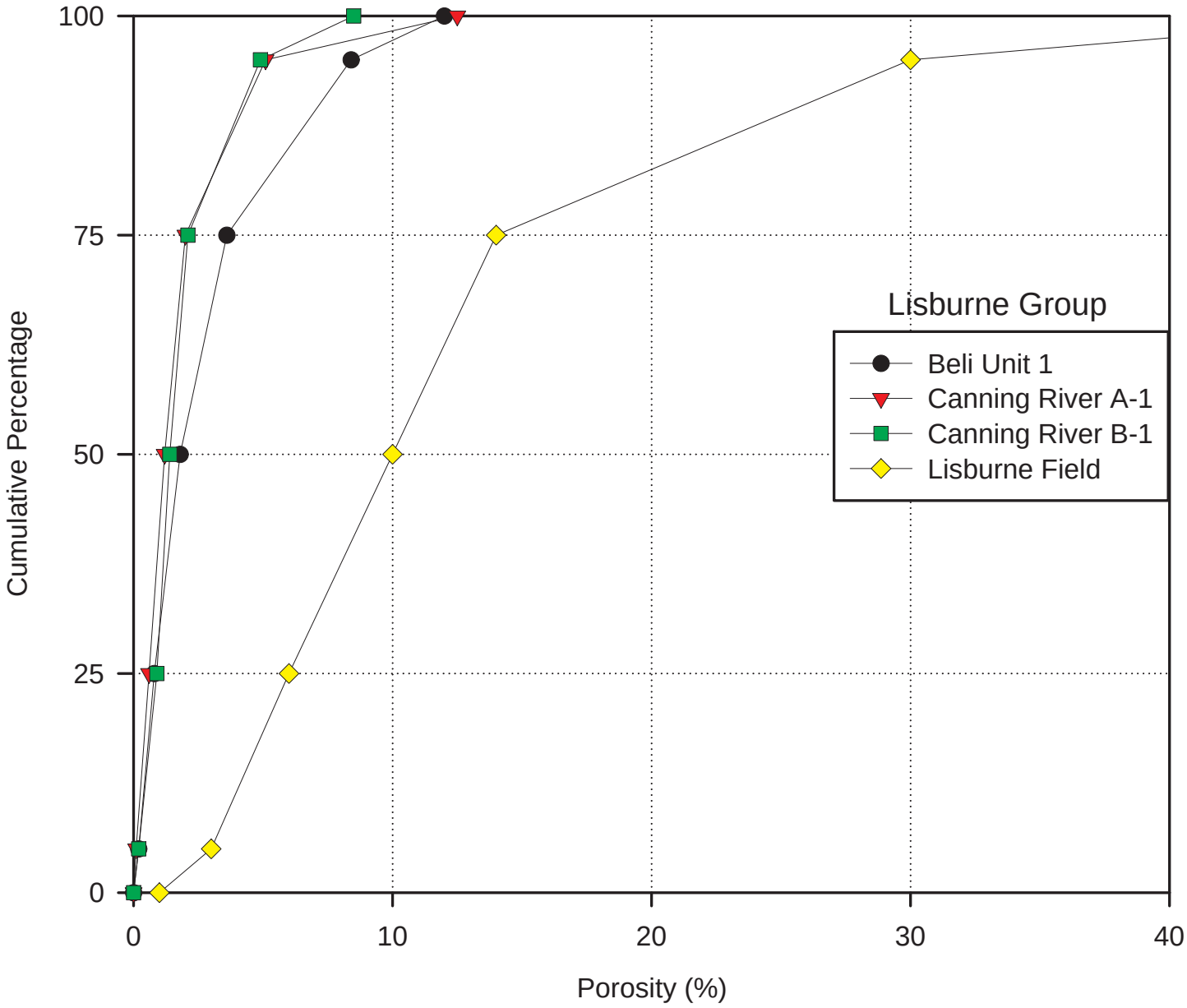

Figure PP1c. Cumulative distributions of porosity from well logs and core data for Lisburne Group.

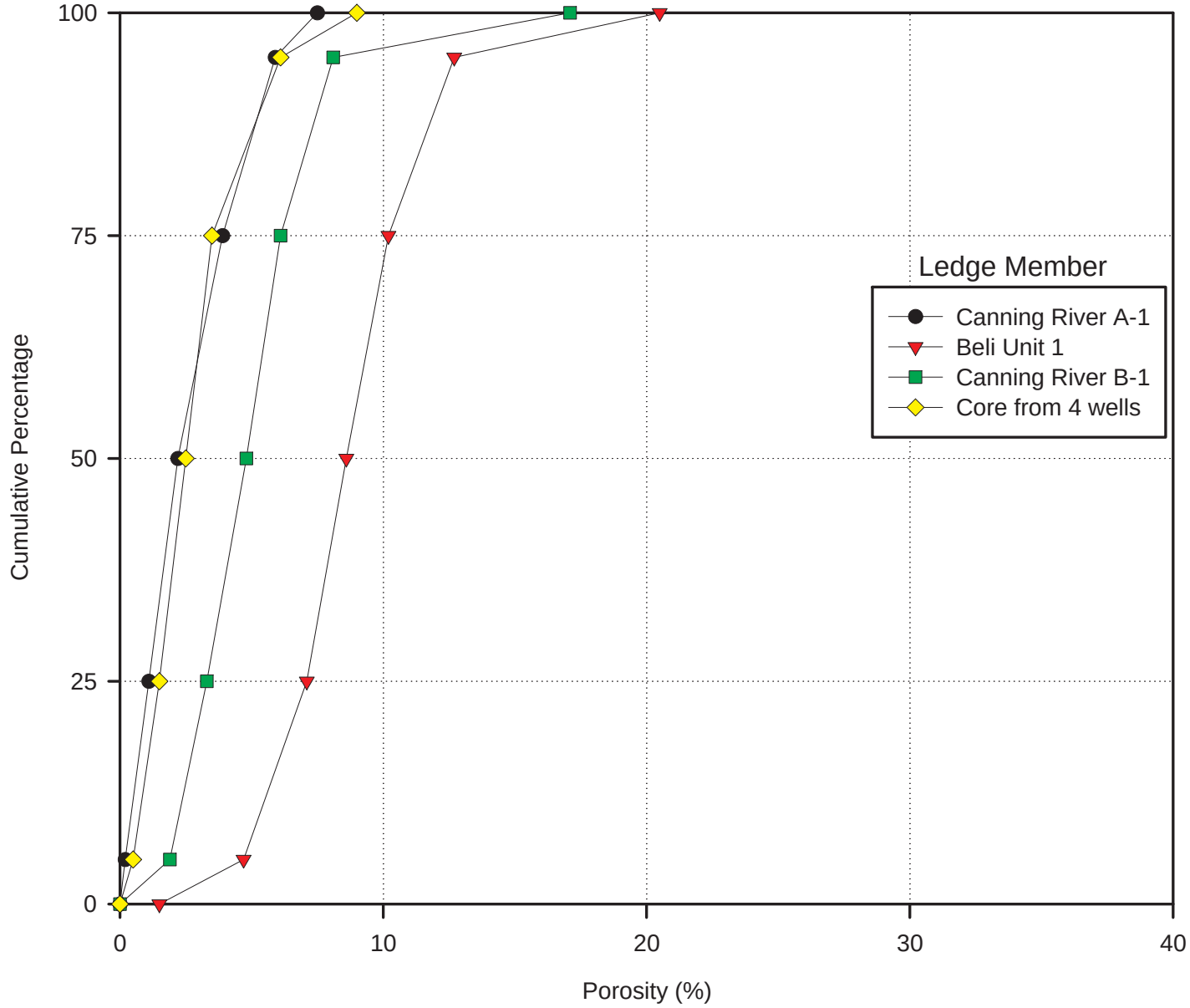

Figure PP1d. Cumulative distributions of porosity from well logs and core samples for Ledge Member.

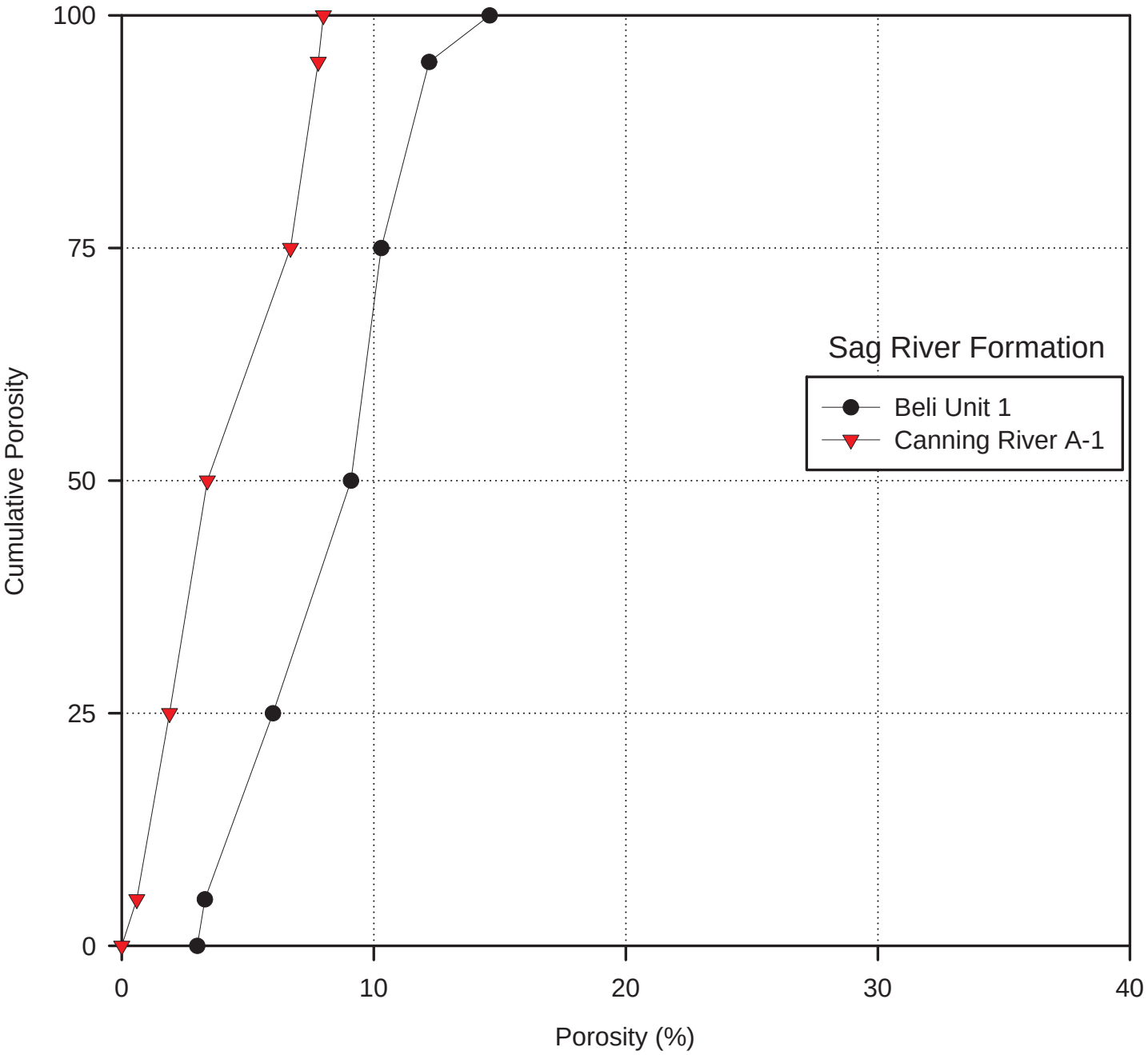

Figure PP1e. Cumulative distributions of porosity from well logs, Sag River Sandstone.

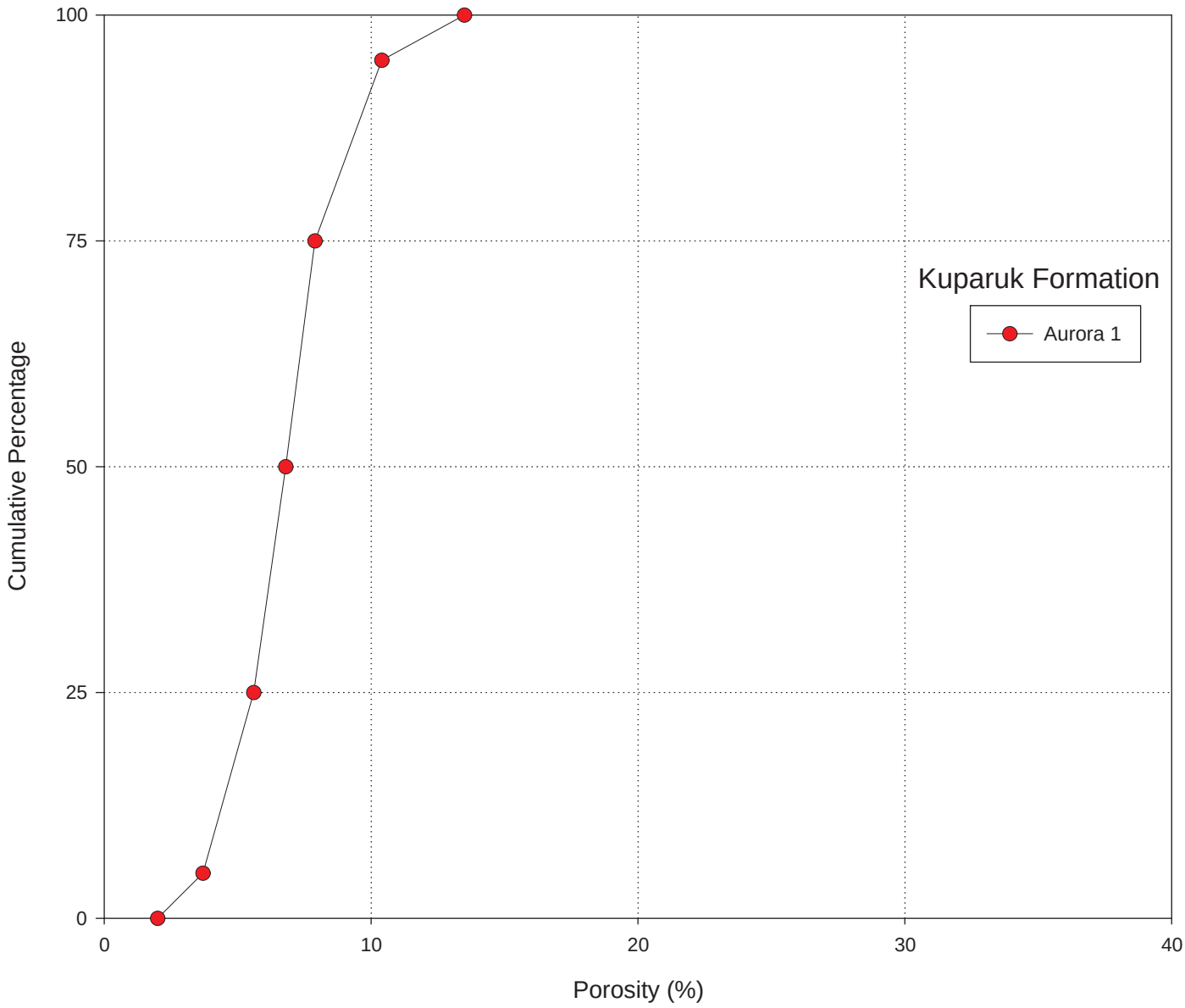

Figure PP1f. Cumulative distributions of porosity from well logs, Kuparuk River Formation.

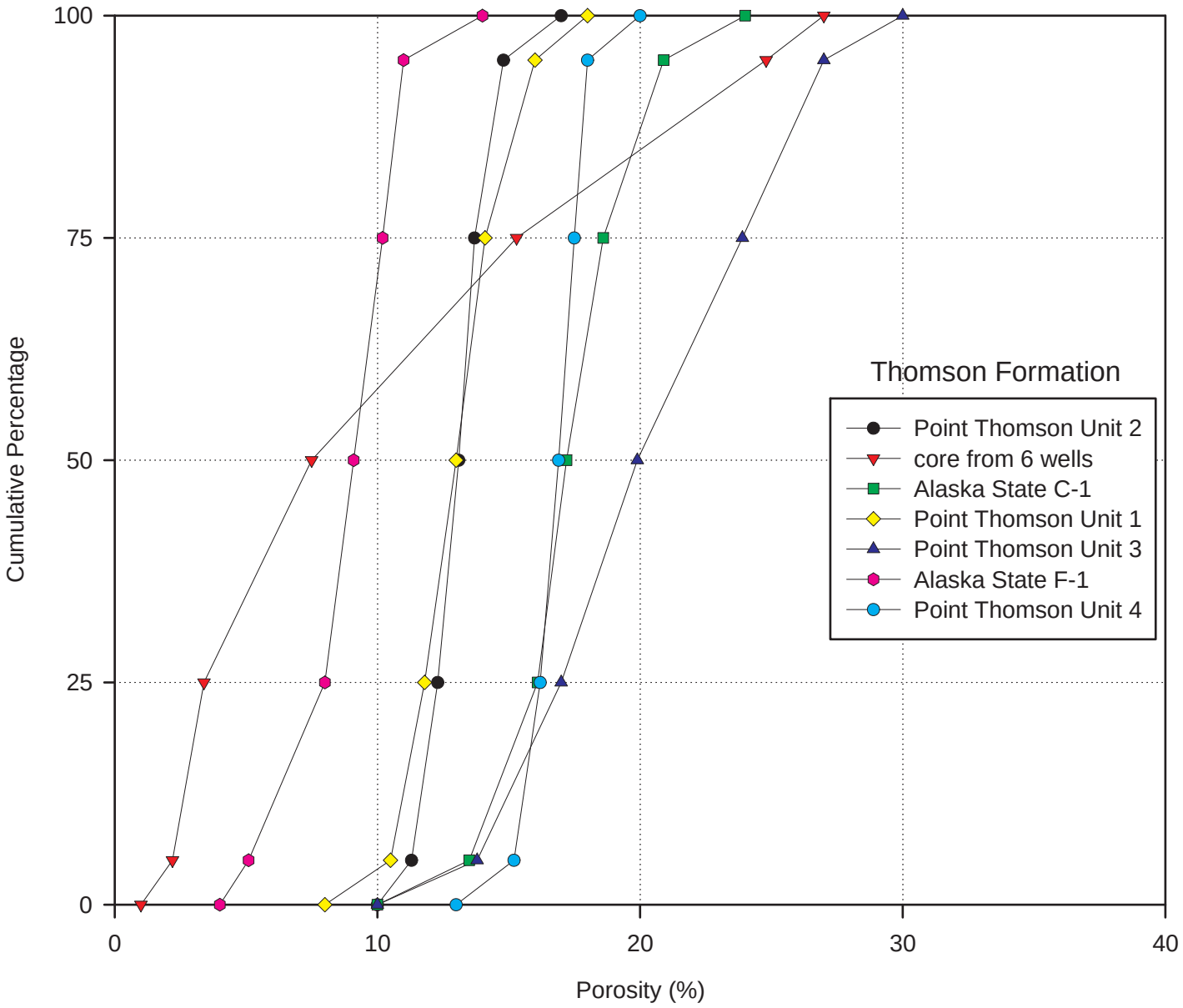

Figure PP1g. Cumulative distributions of porosity from well logs and core samples, Thomson Sand.

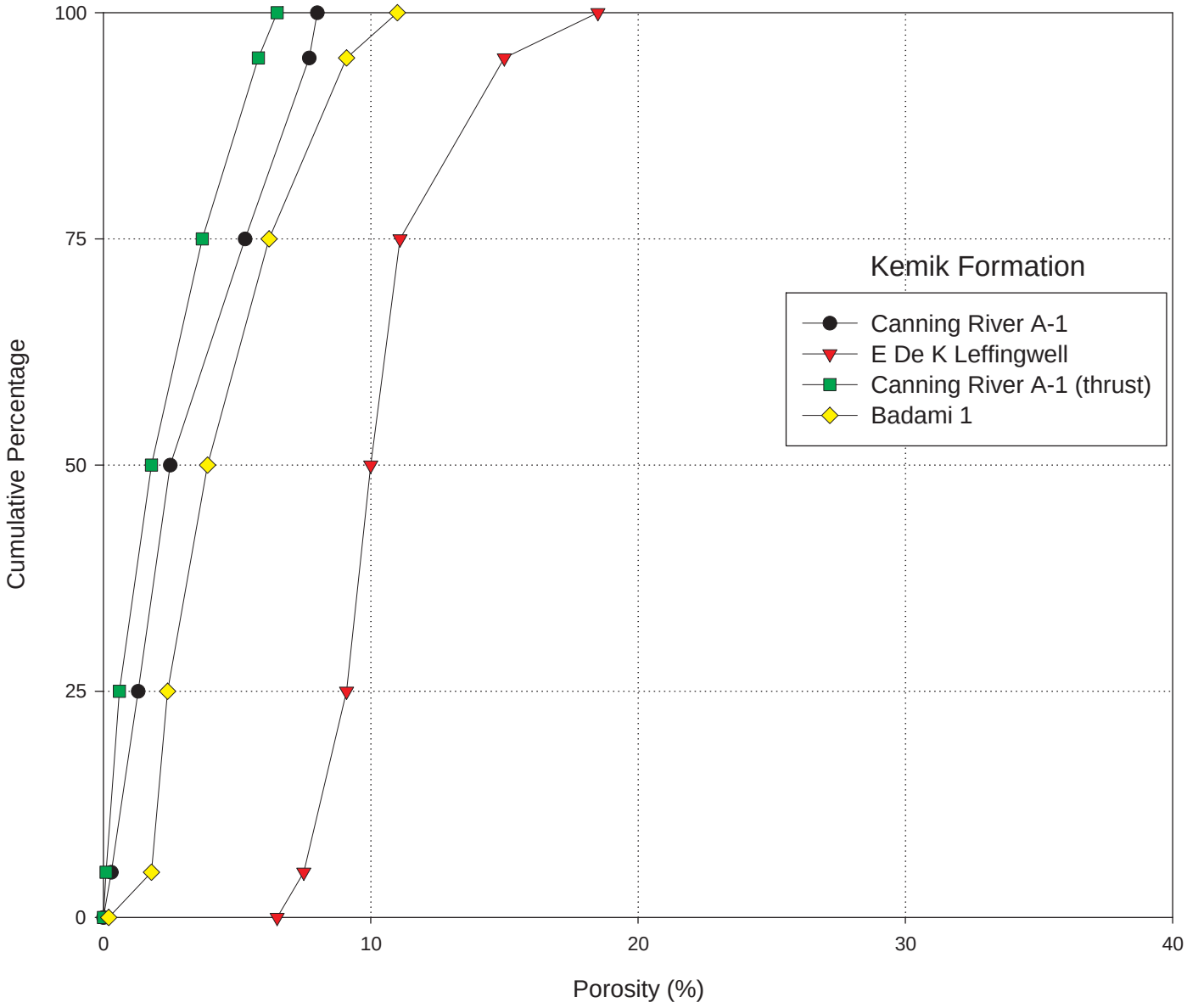

Figure PP1h. Cumulative distributions of porosity from well logs and core samples, Kemik Sandstone.

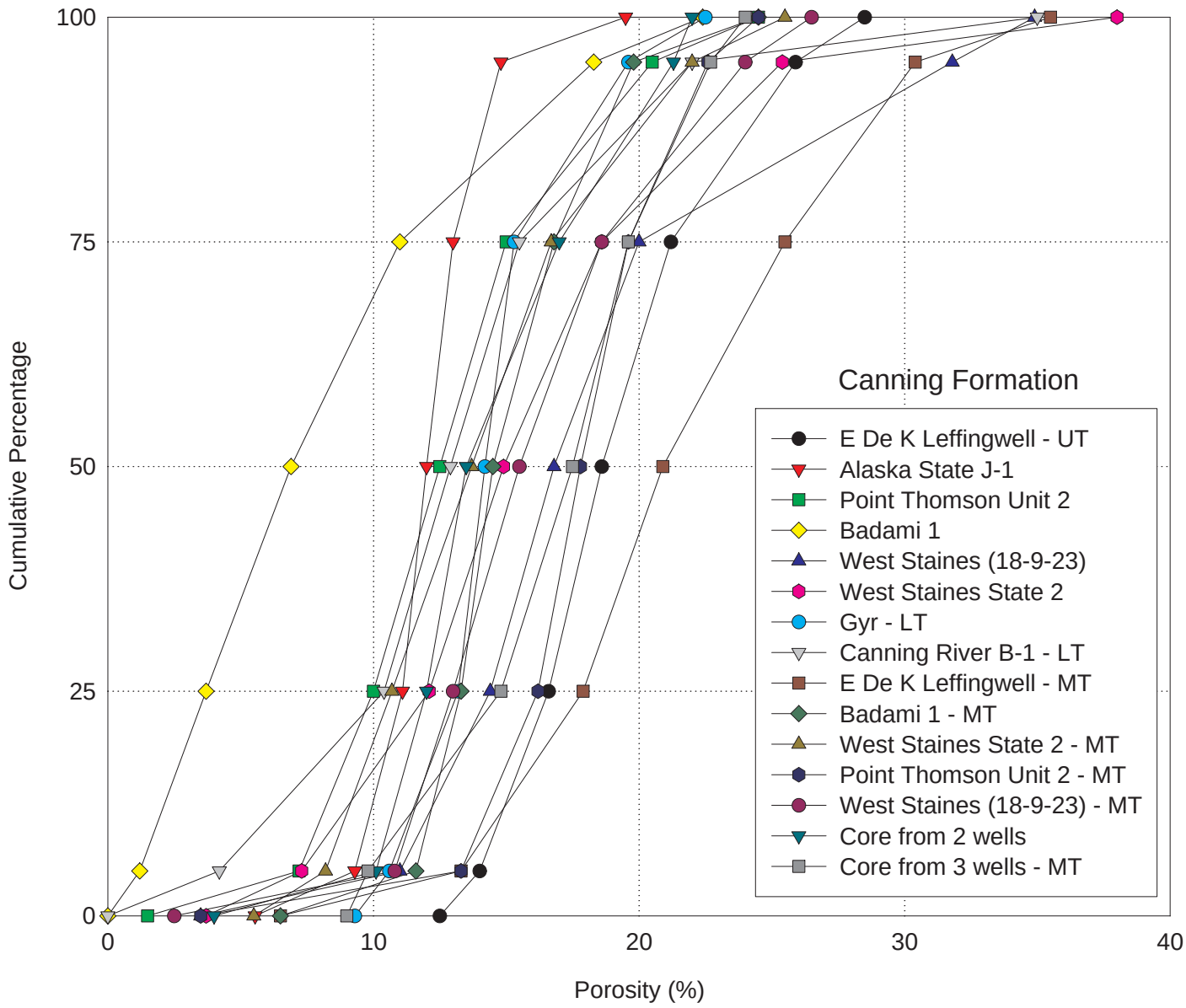

Figure PP1i. Cumulative porosity distribution for Canning Formation.
UT - upper tongue, LT - lower tongue, MT - Mikkelsen Tongue.

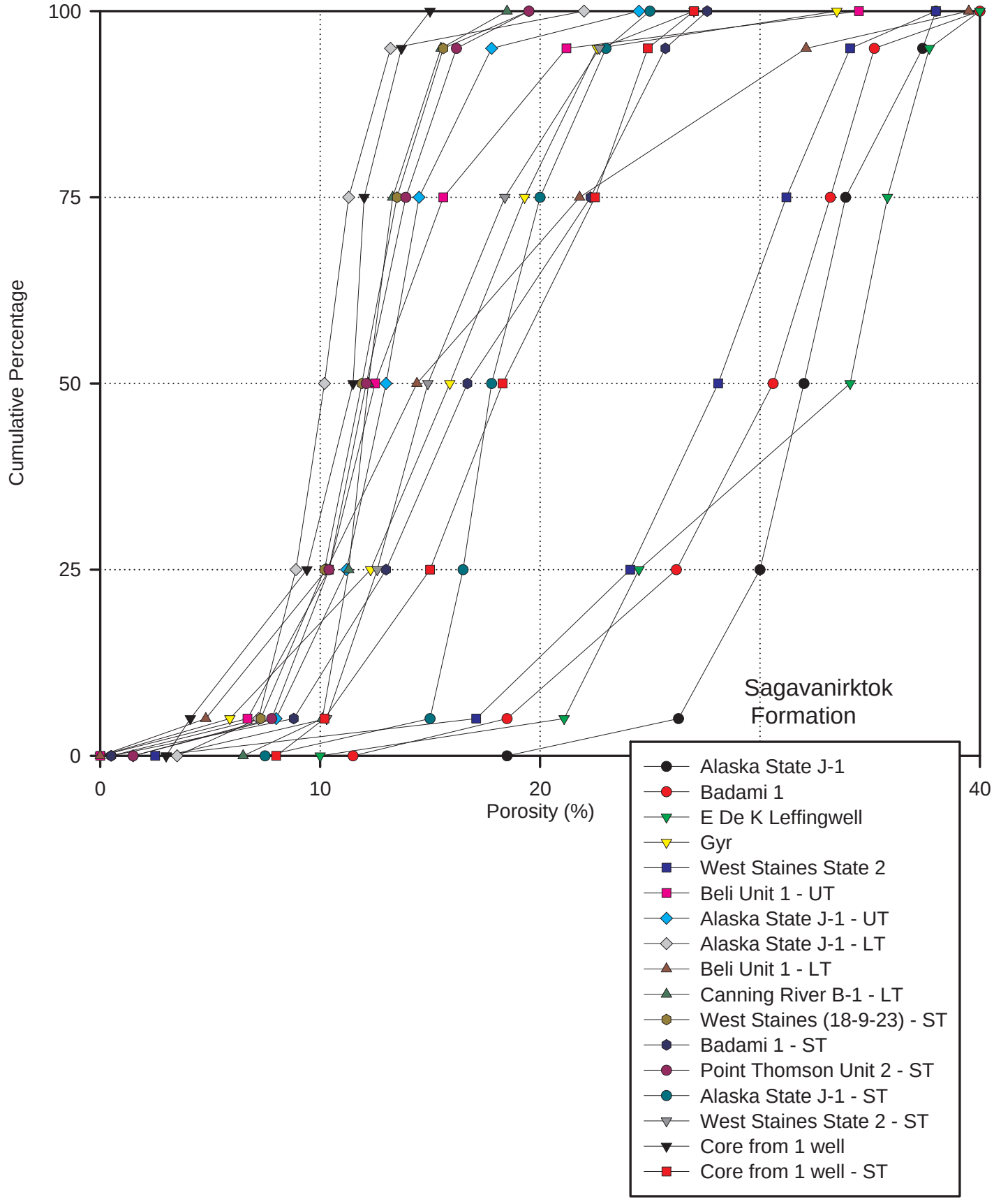

Figure PP1j. Cumulative porosity distribution for Sagavanirktok Formation. UT - upper tongue, LT - lower tongue, ST - Staines Tongue.

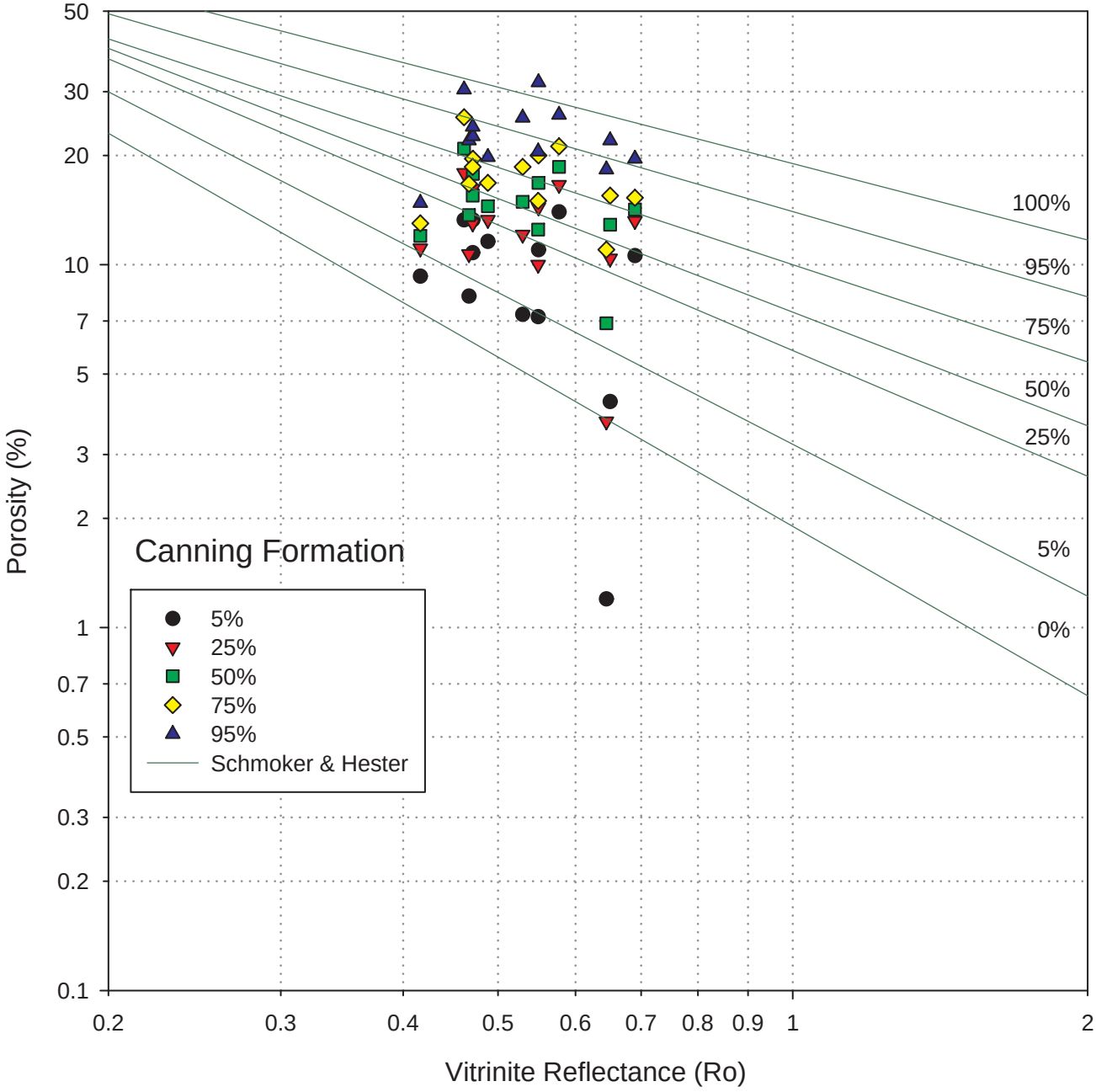

Figure PP2. Canning Formation. Porosity, sampled from cumulative distributions of Fig. PP1i, against vitrinite reflectance (Ro). Solid lines represent relationships established by Schmoker and Hester (1990).

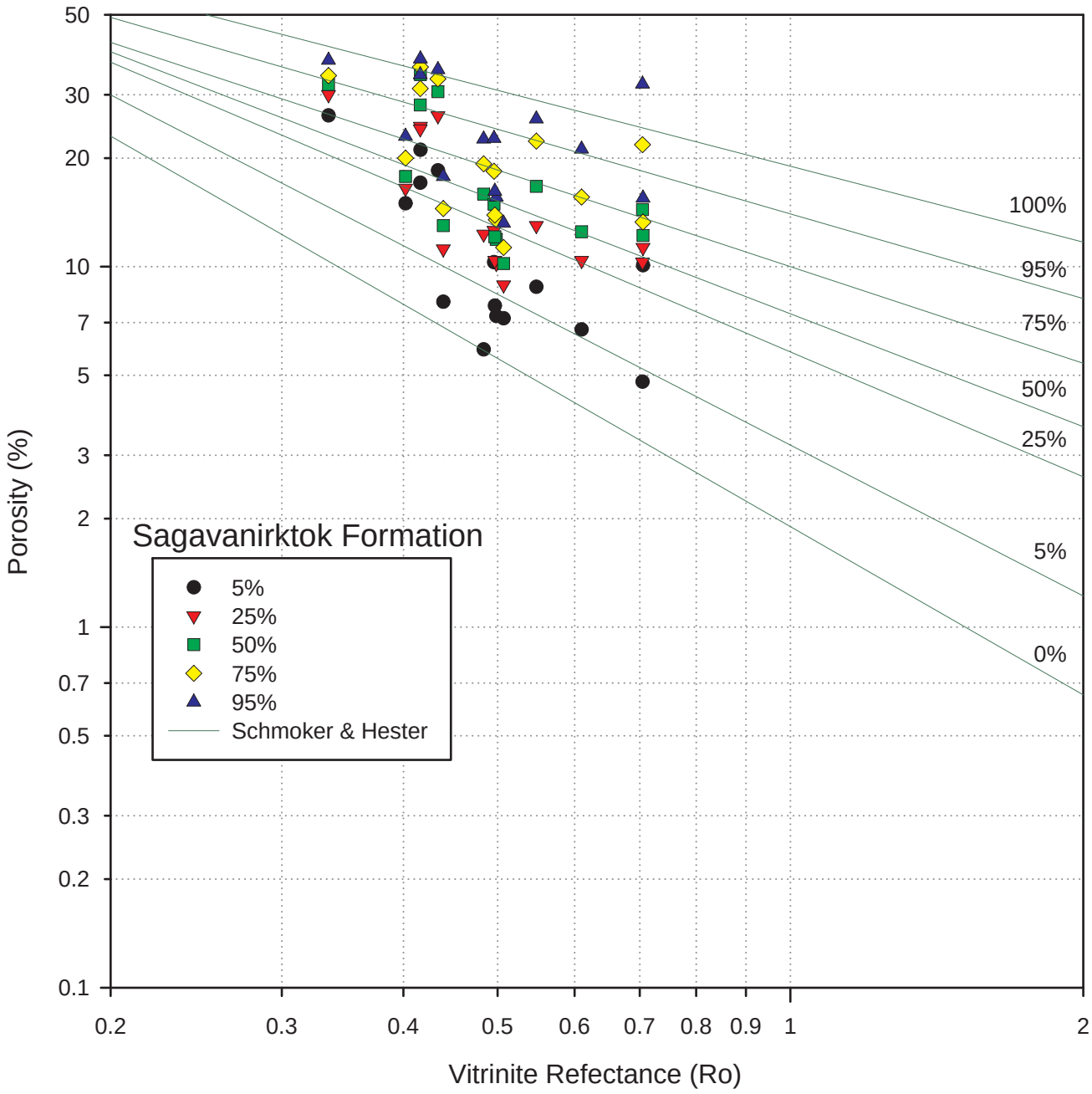

Figure PP3. Sagavanirktok Formation. Porosity, sampled from cumulative distributions of Fig. PP1j, against vitrinite reflectance (Ro). Solid lines represent relationships established by Schmoker and Hester (1990).

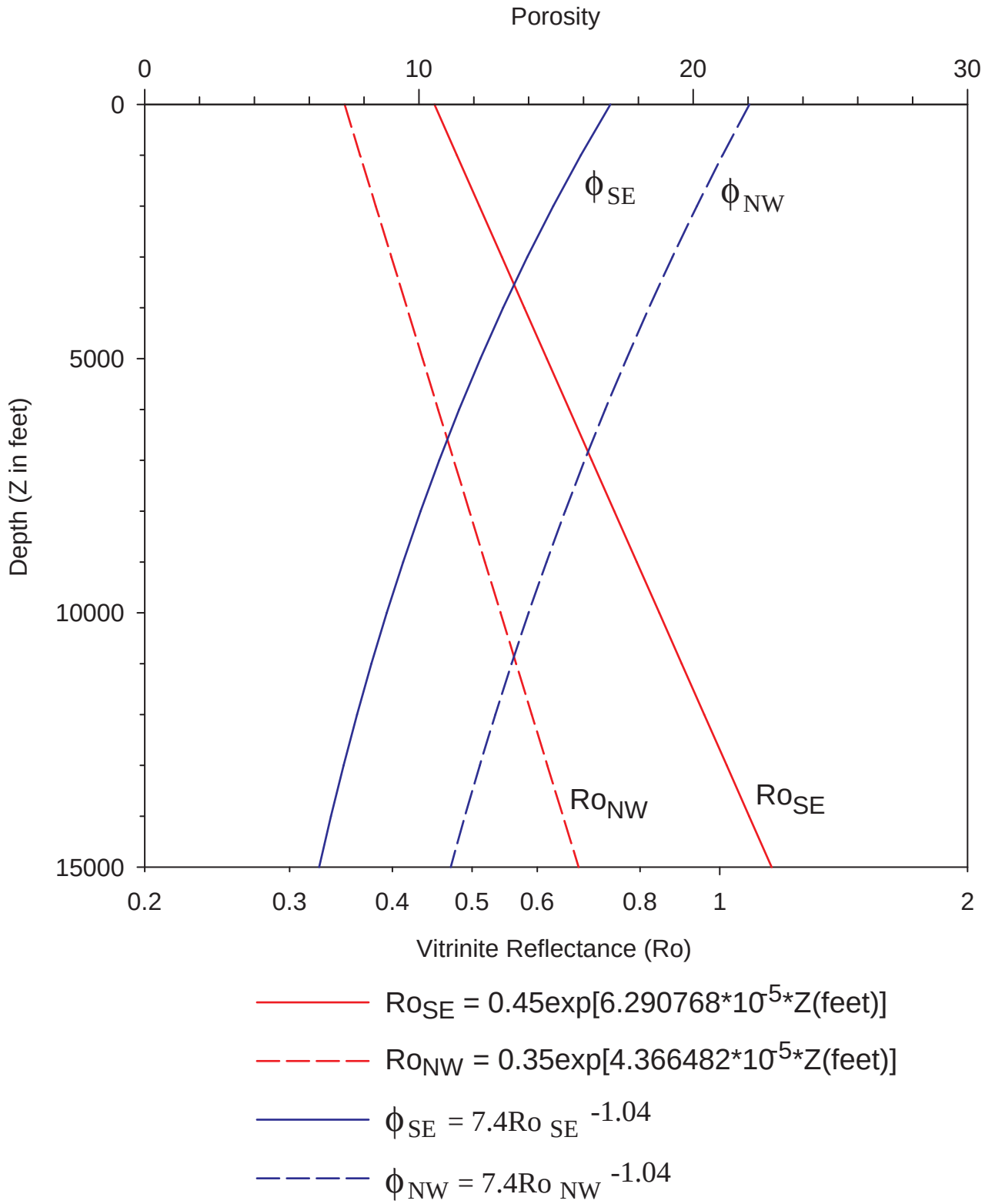

Figure PP4. Porosity and vitrinite reflectance (Ro) as functions of depth (Z). Vitrinite reflectance subscripted SE applies southeast of Marsh Creek Anticline; the subscript NW applies to the northwest. The two corresponding porosity curves are for the 50th percentile of the Canning and Sagavanirktok Formations, using the A,B coefficients given in Table PP6.

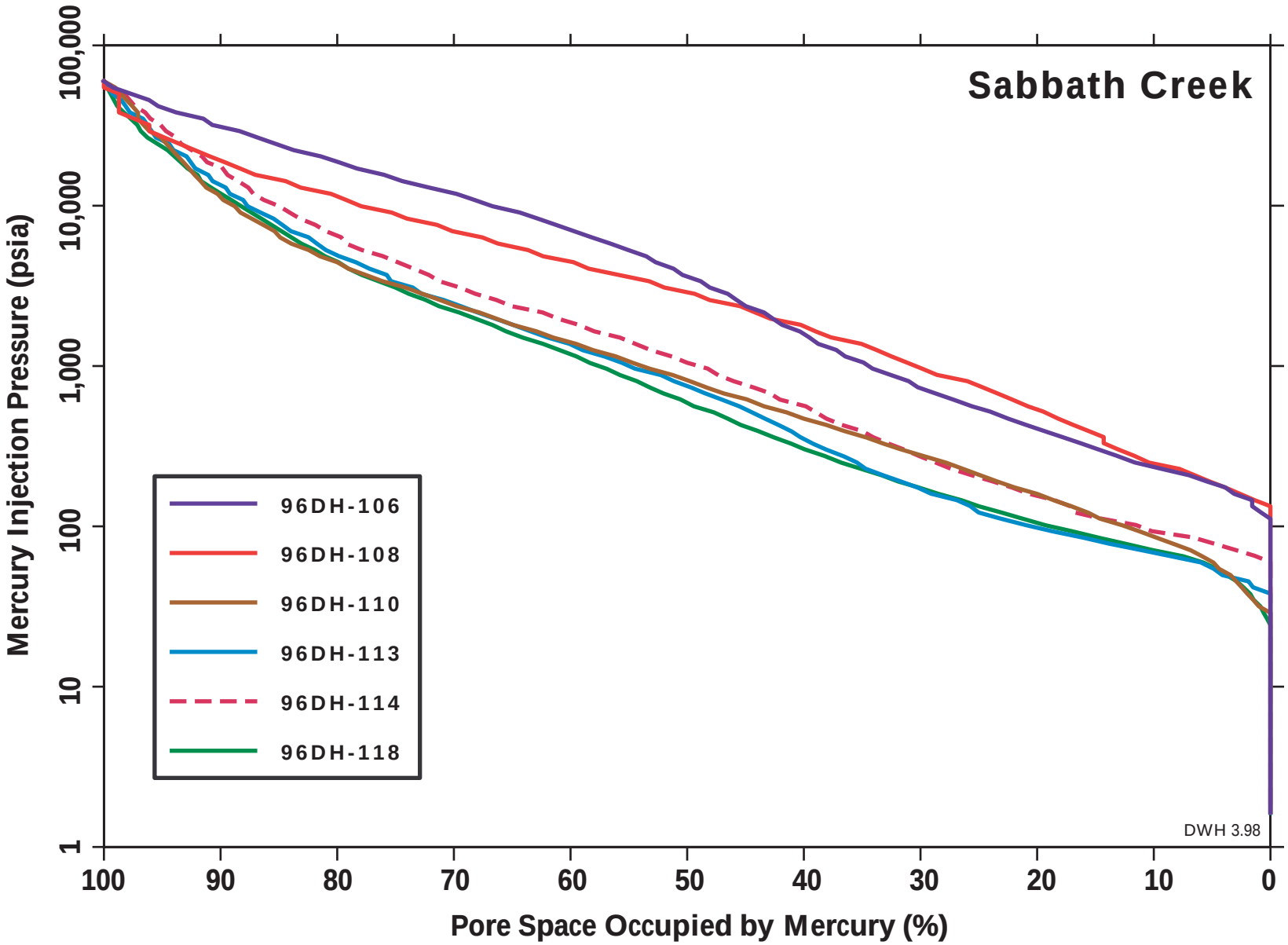

Figure PP5a. Capillary pressure (logarithmic scale) by mercury injection, Sabbath Creek Formation. All samples are surface samples

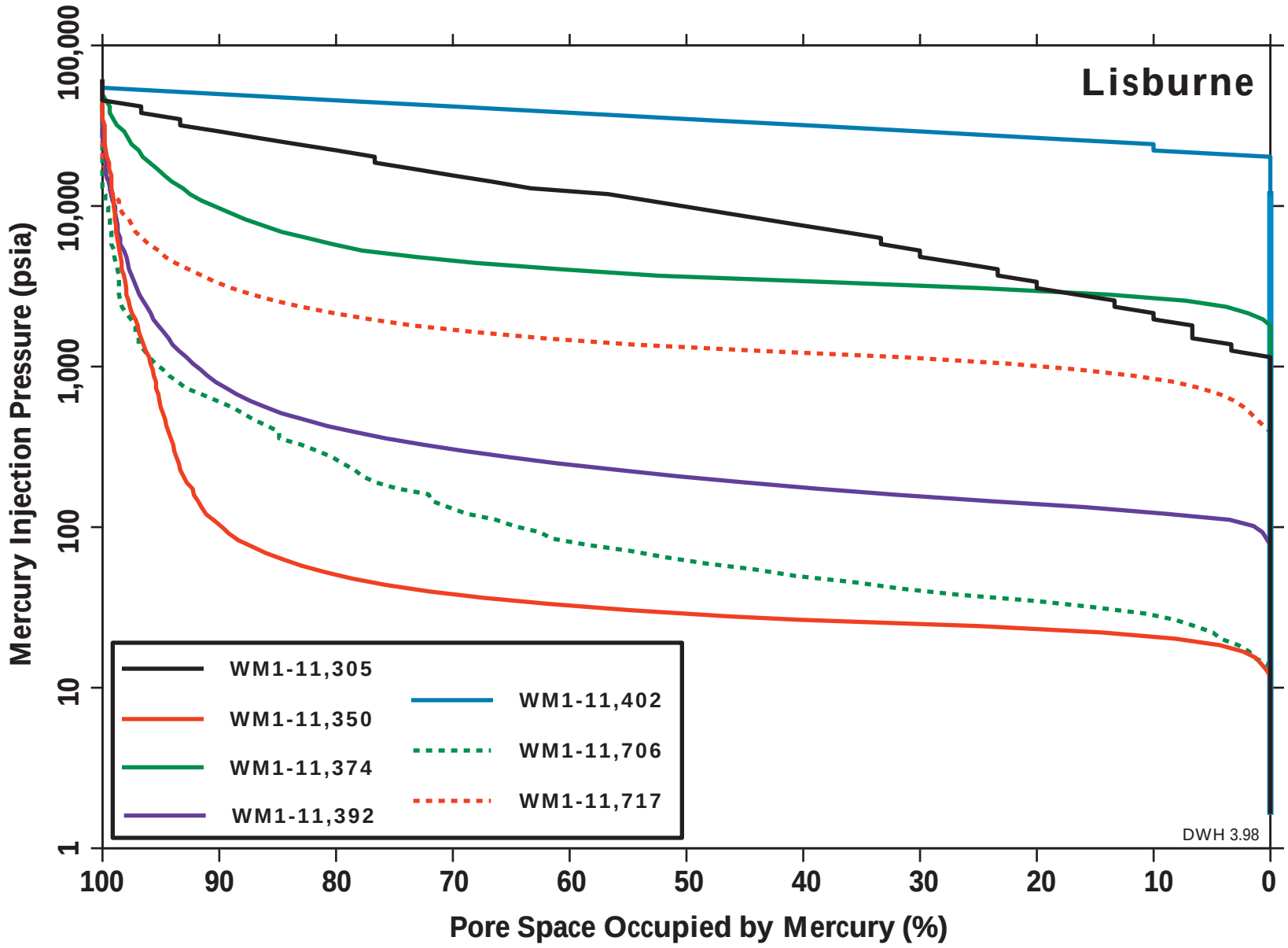

Figure PP5b. Capillary pressure (logarithmic scale) by mercury injection, Lisburne Formation. All samples are from well West Mikkelsen State 1

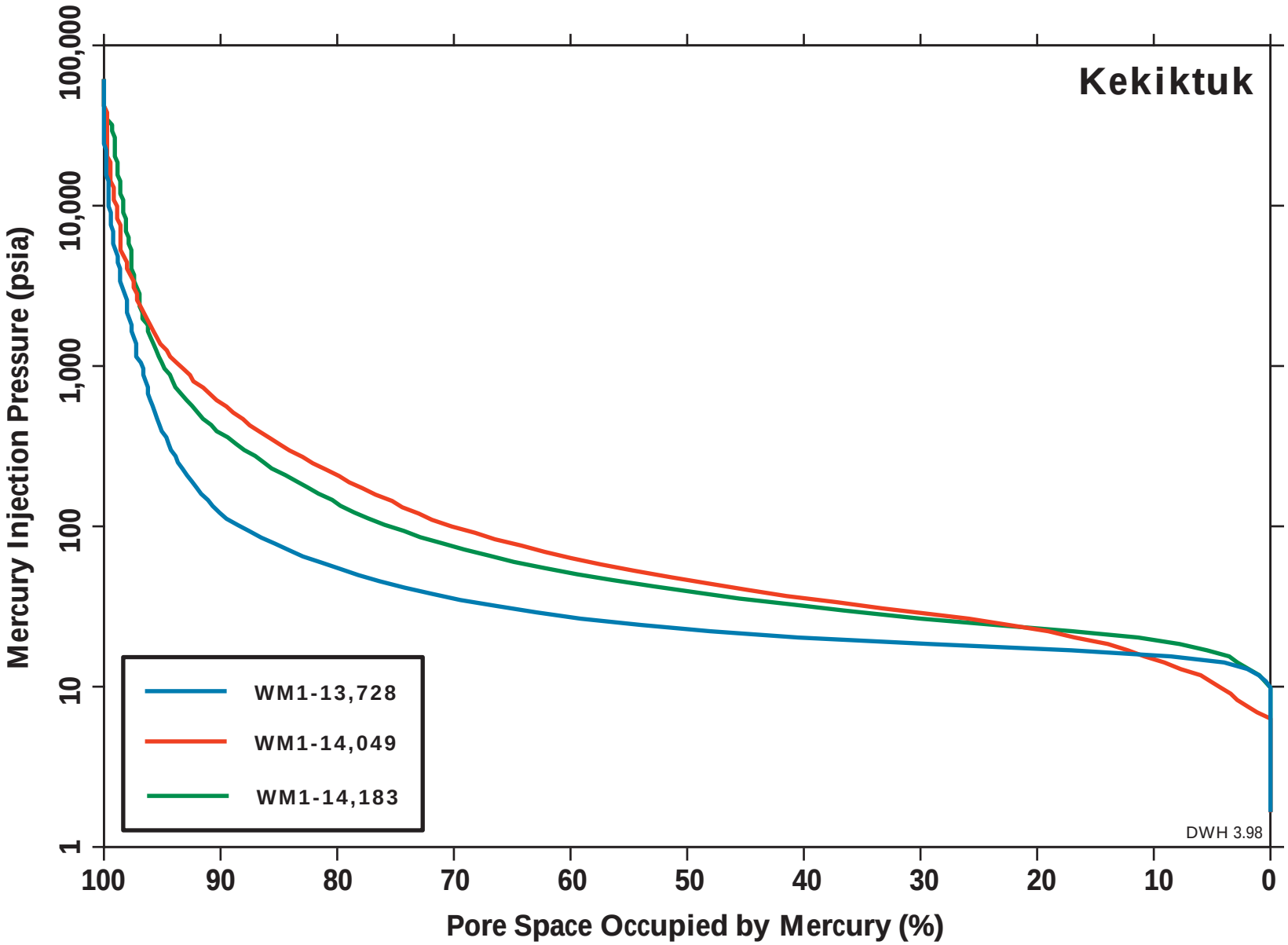

Figure PP5c. Capillary pressure (logarithmic scale) by mercury injection, Kekiktuk Formation. Samples are from well West Mikkelsen State 1.

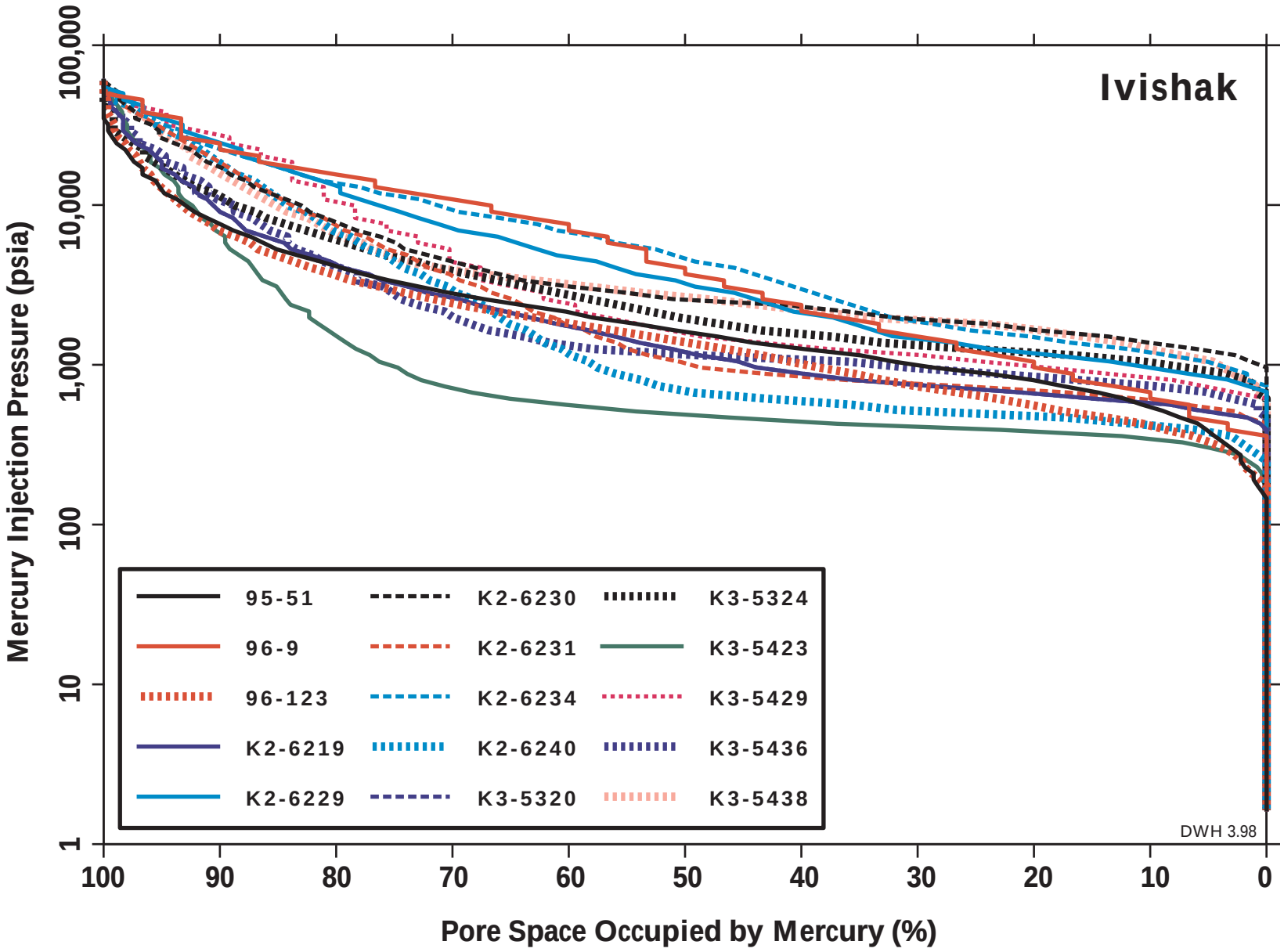

Figure PP5d. Capillary pressure (logarithmic scale) by mercury injection, Ivishak Formation. Samples with K2 and K3 prefix are from wells Kavik Unit 2 and Kavik Unit 3. Samples with prefix 95 and 96 are surface samples.

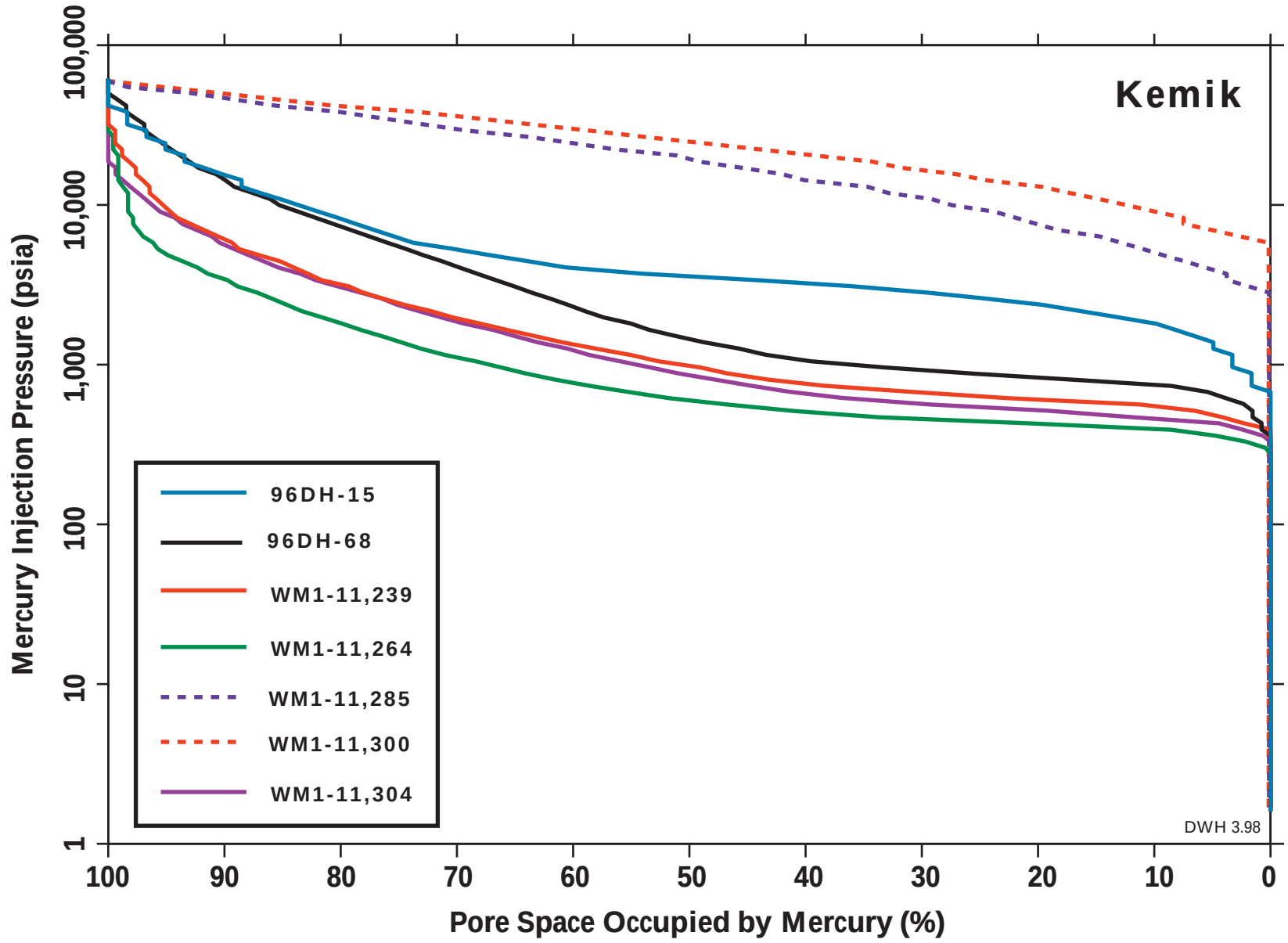

Figure PP5e. Capillary pressure (logarithmic scale) by mercury injection, Kemik Sandstone. Samples with WM1 prefix are from well West Mikkelsen State 1 Samples with 96 prefix are surface samples.

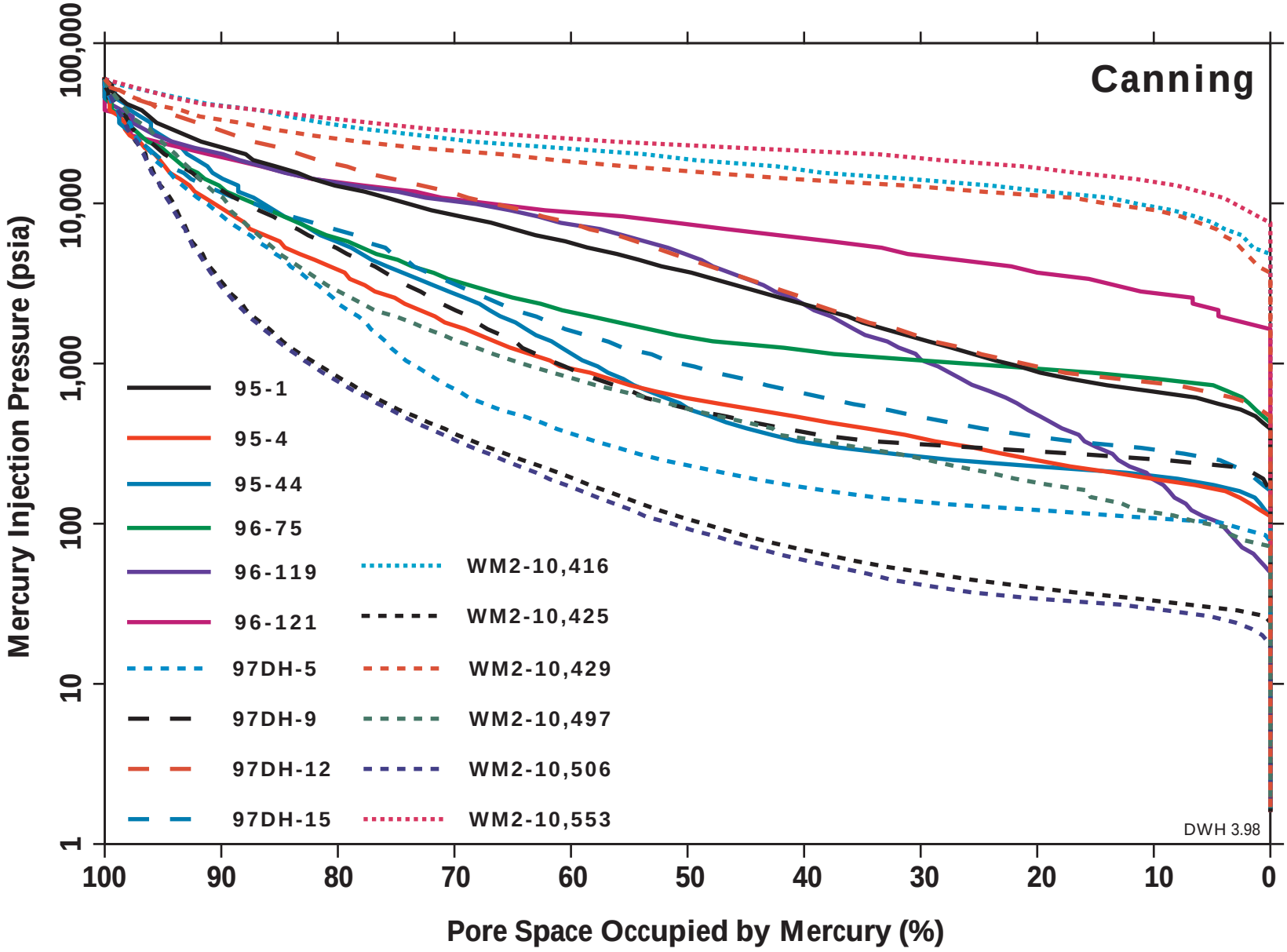

Figure PP5f. Capillary pressure (logarithmic scale) by mercury injection, Canning Formation. Samples with prefix WM2 are from well West Mikkelsen Unit 2. Samples with 95, 96, and 97 prefix are surface samples.

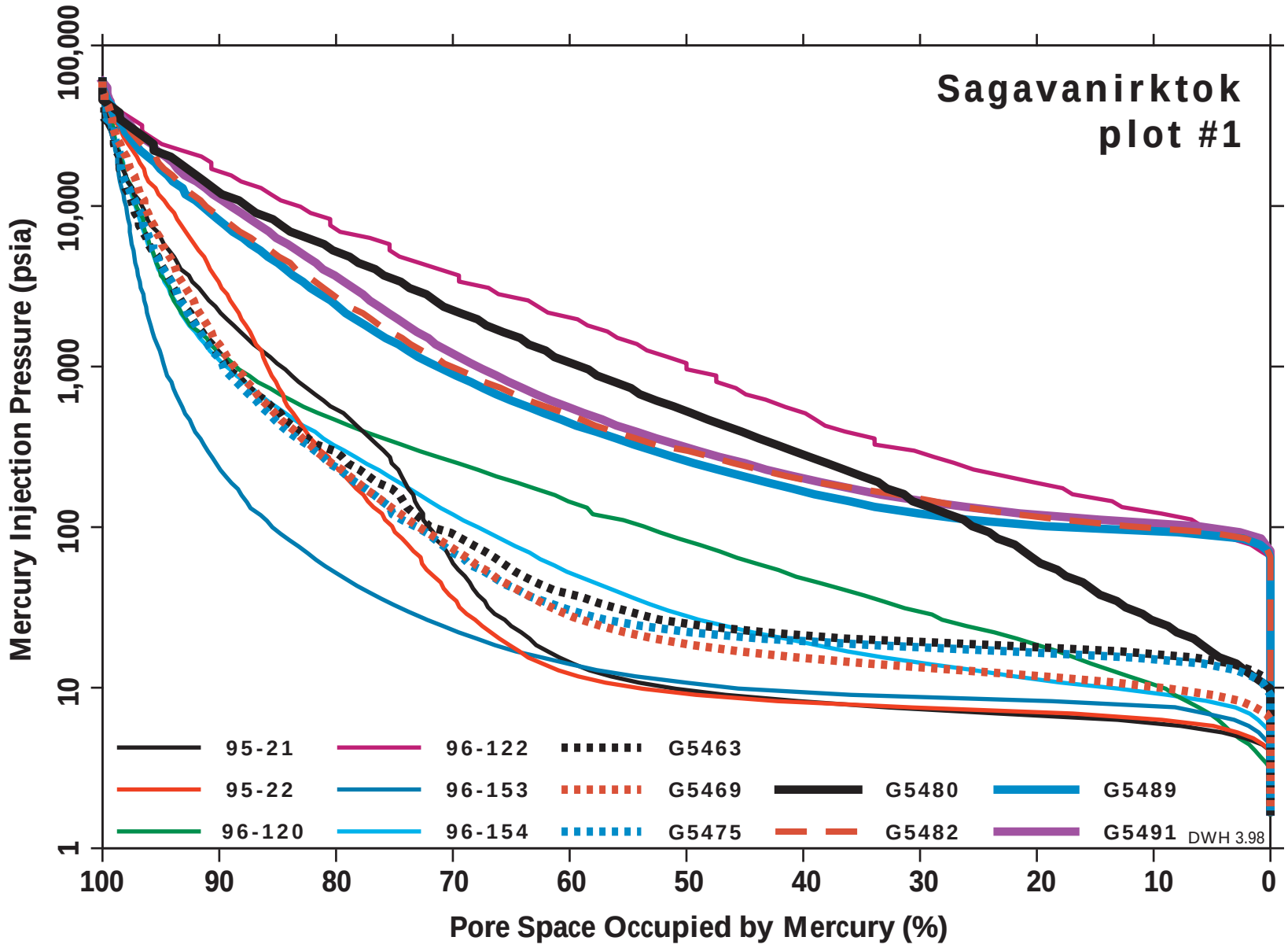

Figure PP5g. Capillary pressure (logarithmic scale) by mercury injection, Sagavanirktok Formation (first of two plots). Samples with prefix G are from Gyr well. Samples with 95 and 96 prefix are surface samples.

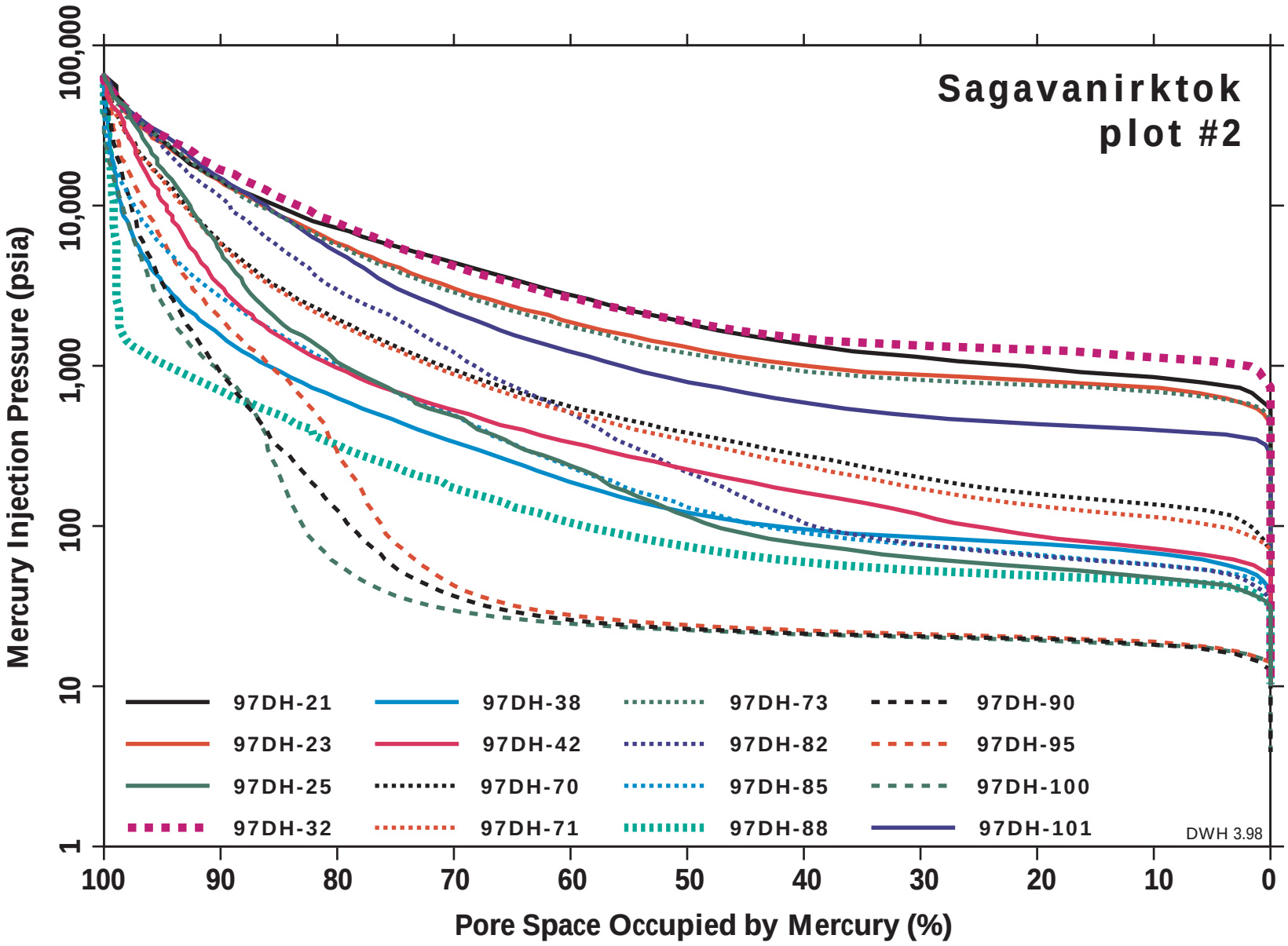

Figure PP5h. Capillary pressure (logarithmic scale) by mercury injection, Sagavanirktok Formation (second of two plots). All samples are surface samples.

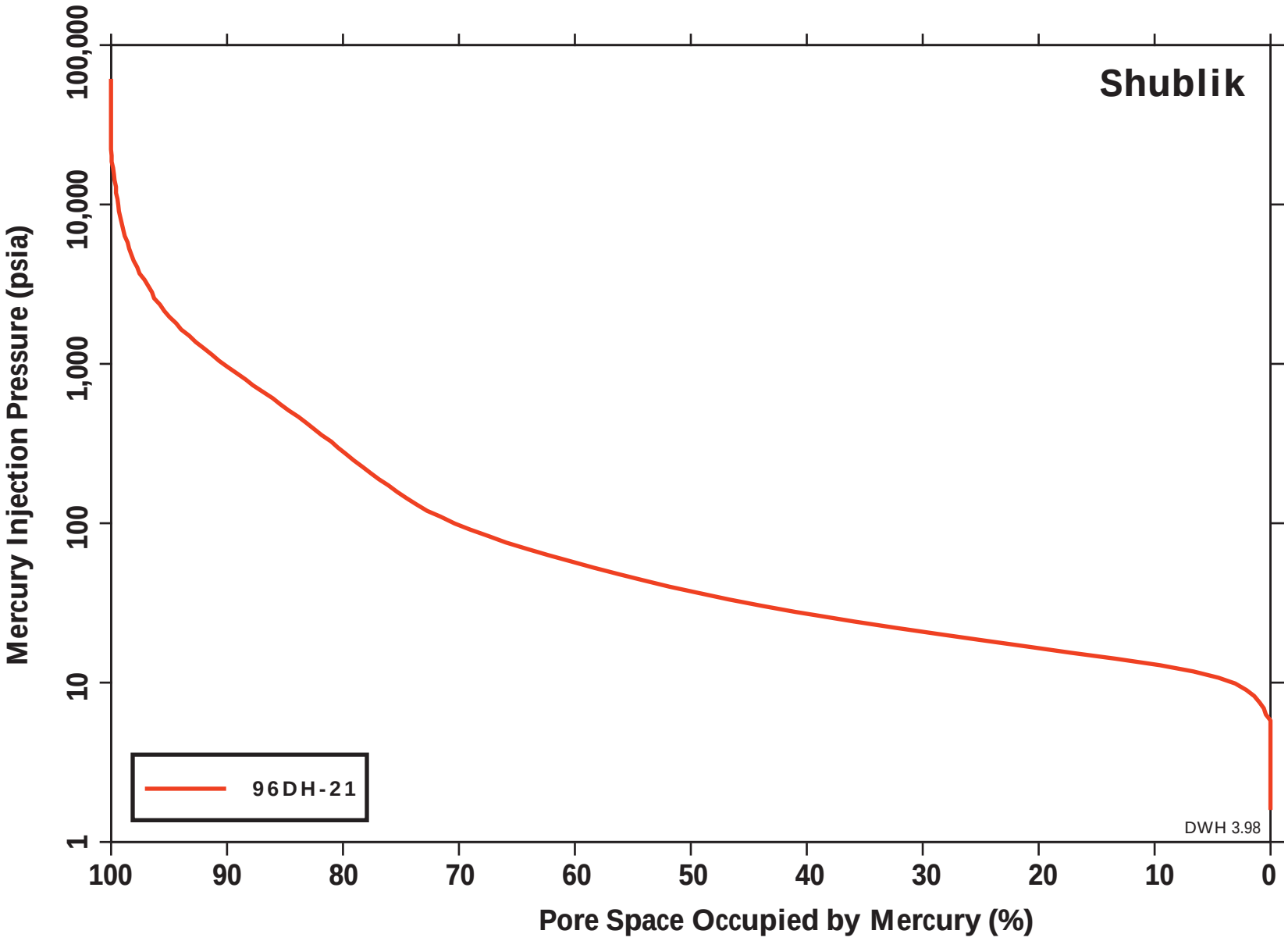

Figure PP5i. Capillary pressure (logarithmic scale) by mercury injection of a single sample from the Shublik Formation.

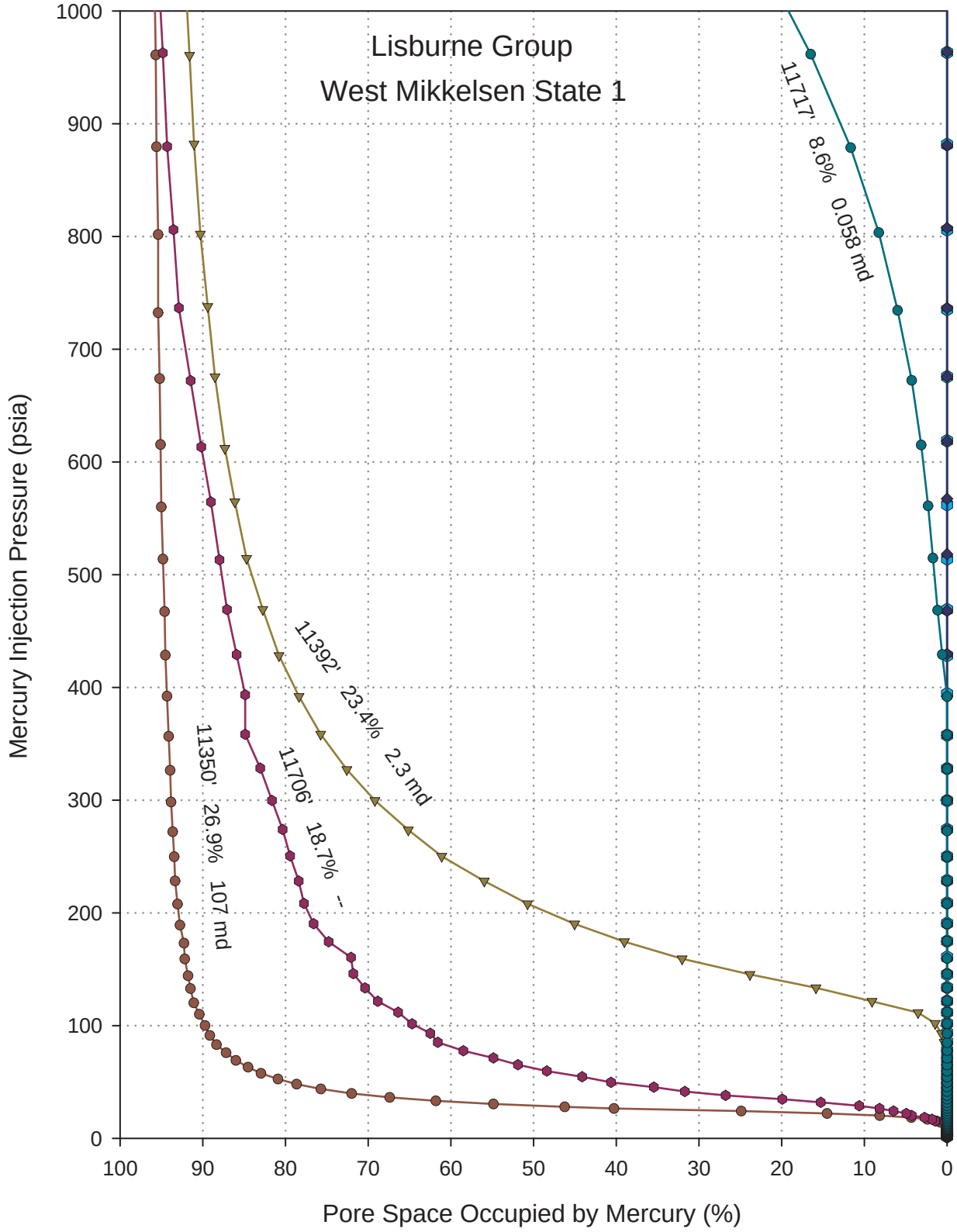

Figure PP6a. Capillary pressure by mercury injection, linear scales, Lisburne Group. All four samples are from well West Mikkelsen State 1.

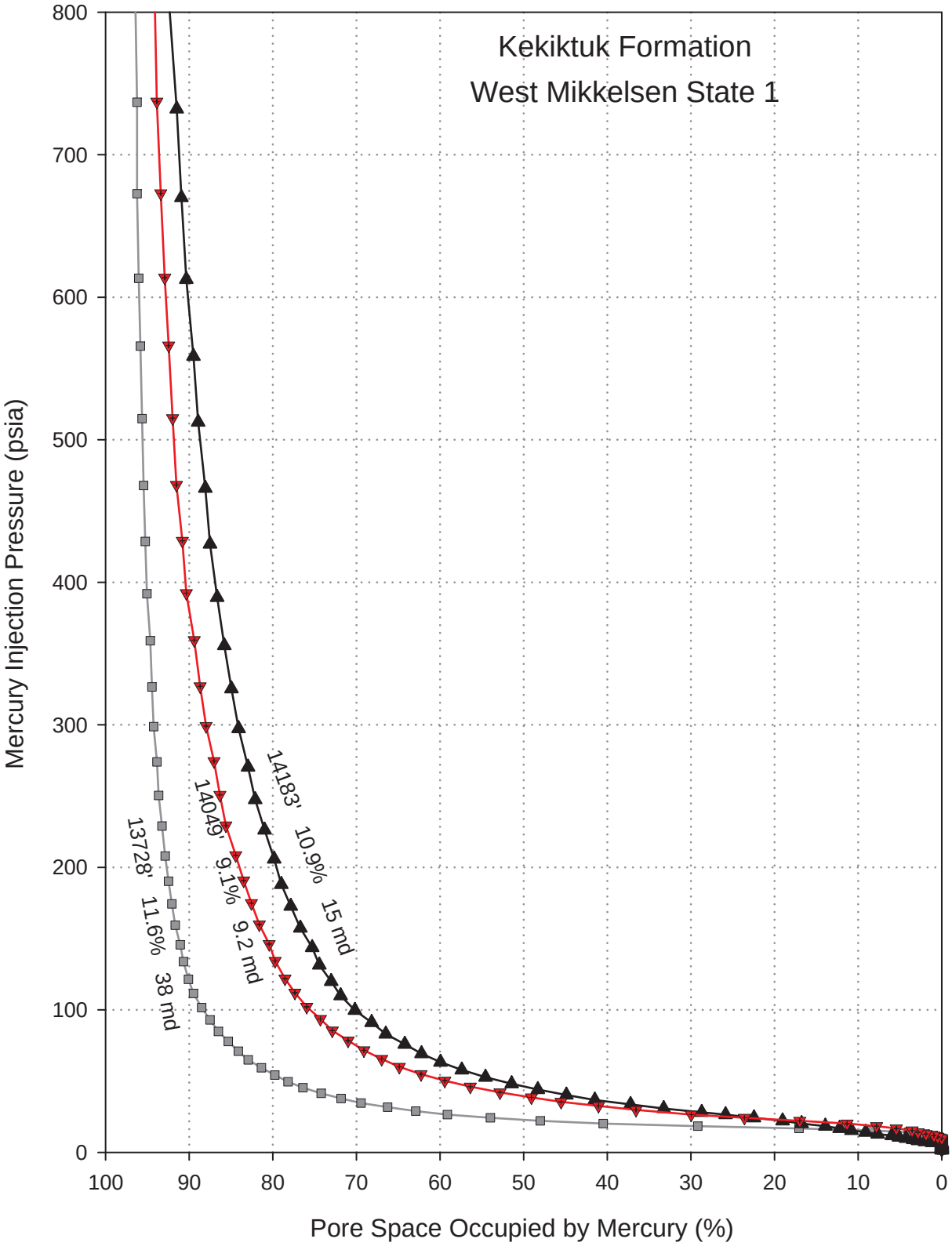

Figure PP6b. Capillary pressure by mercury injection, linear scales, Kekiktuk Formation. Three samples are from well West Mikkelsen State 1.

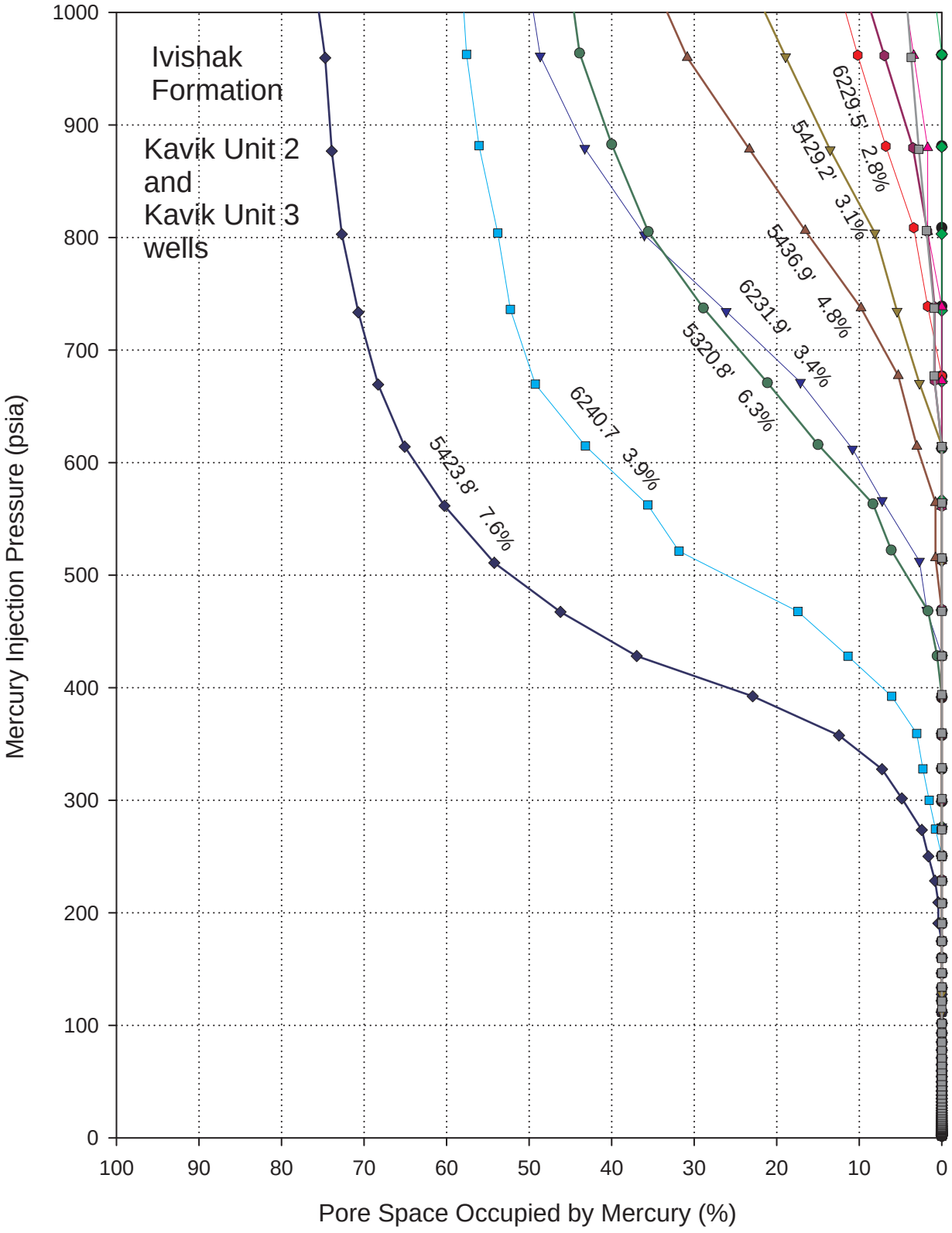

Figure PP6c. Capillary pressure by mercury injection, linear scales, Ivishak Formation. Samples are from Kavik Unit 2 and Kavik Unit 3 wells.

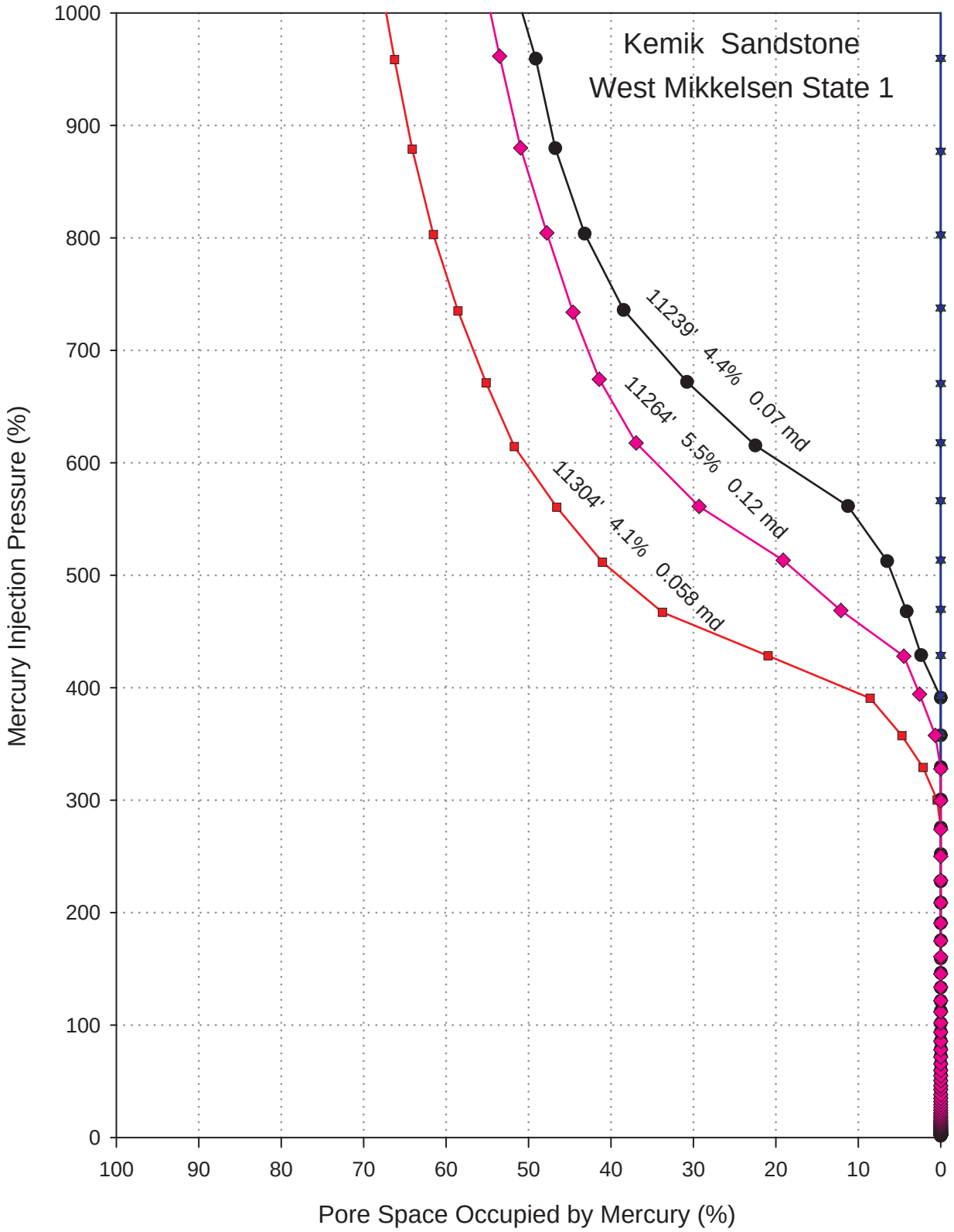

Figure PP6d. Capillary pressure by mercury injection, linear scales, Kemik Sandstone. Three samples are from well West Mikkelsen State 1.

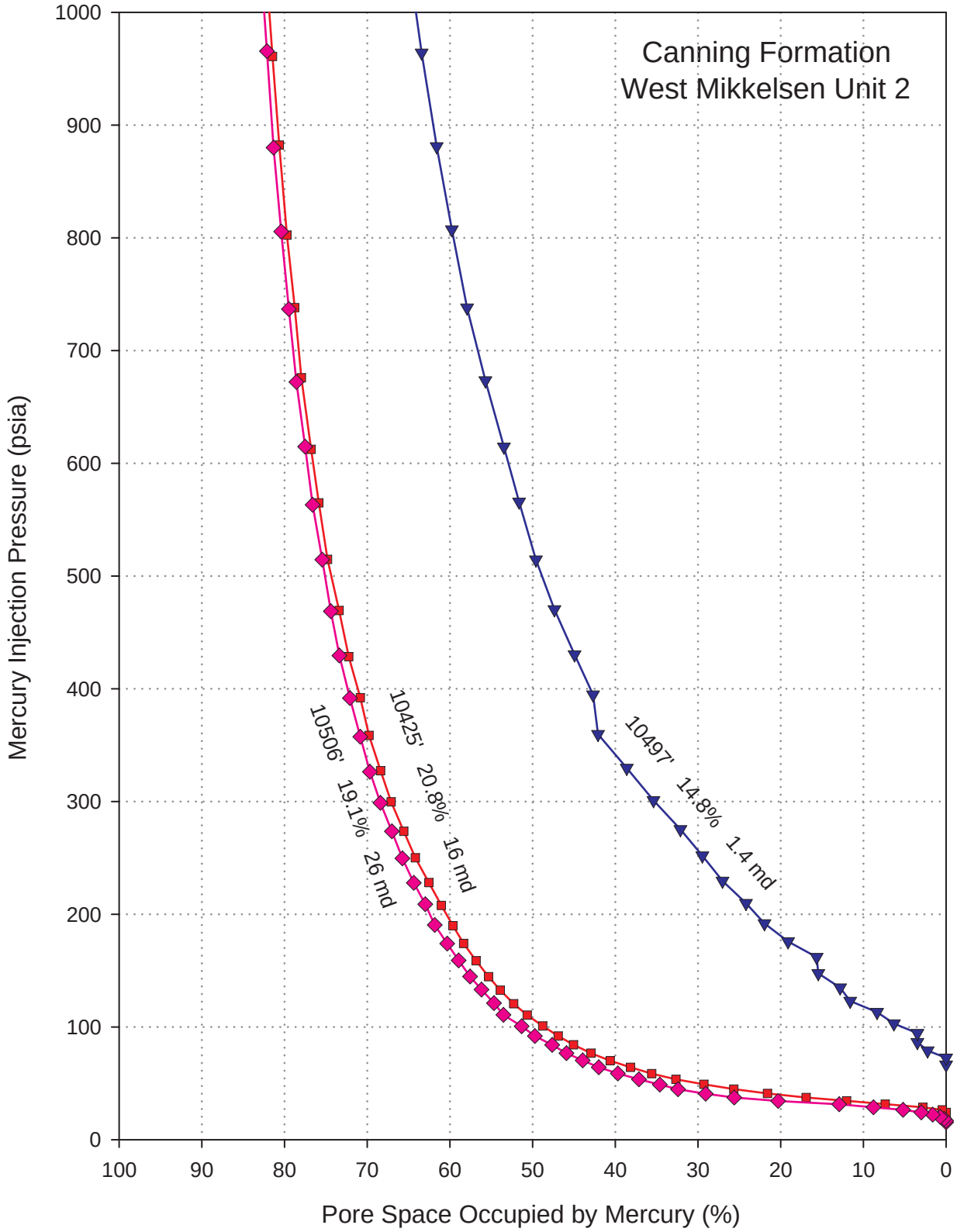

Figure PP6e. Capillary pressure by mercury injection, linear scales, Canning Formation. Three samples are from well West Mikkelsen Unit 2.

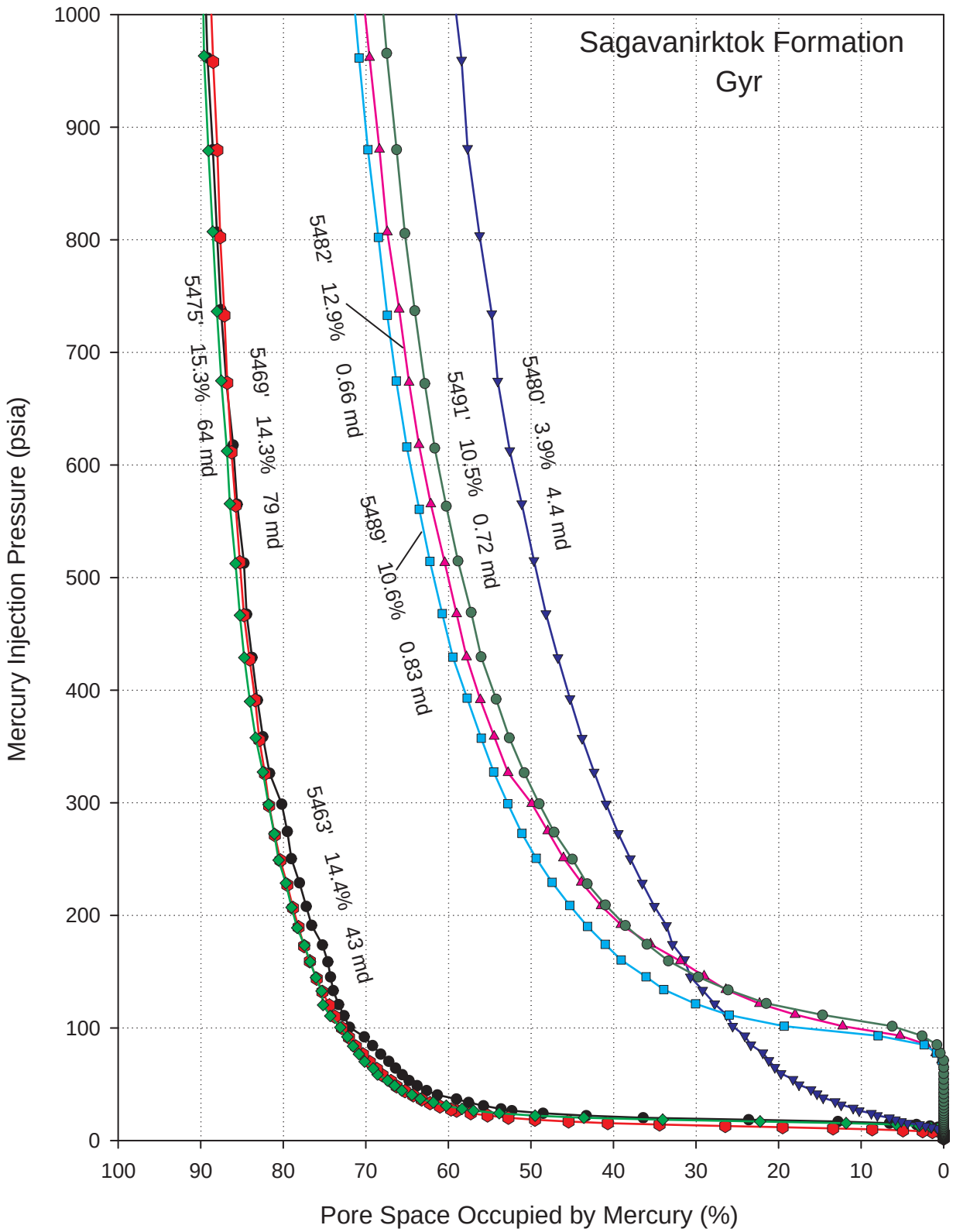

Figure PP6f. Capillary pressure by mercury injection, linear scales, Sagavanirktok Formation. Seven samples are from Gyr well.

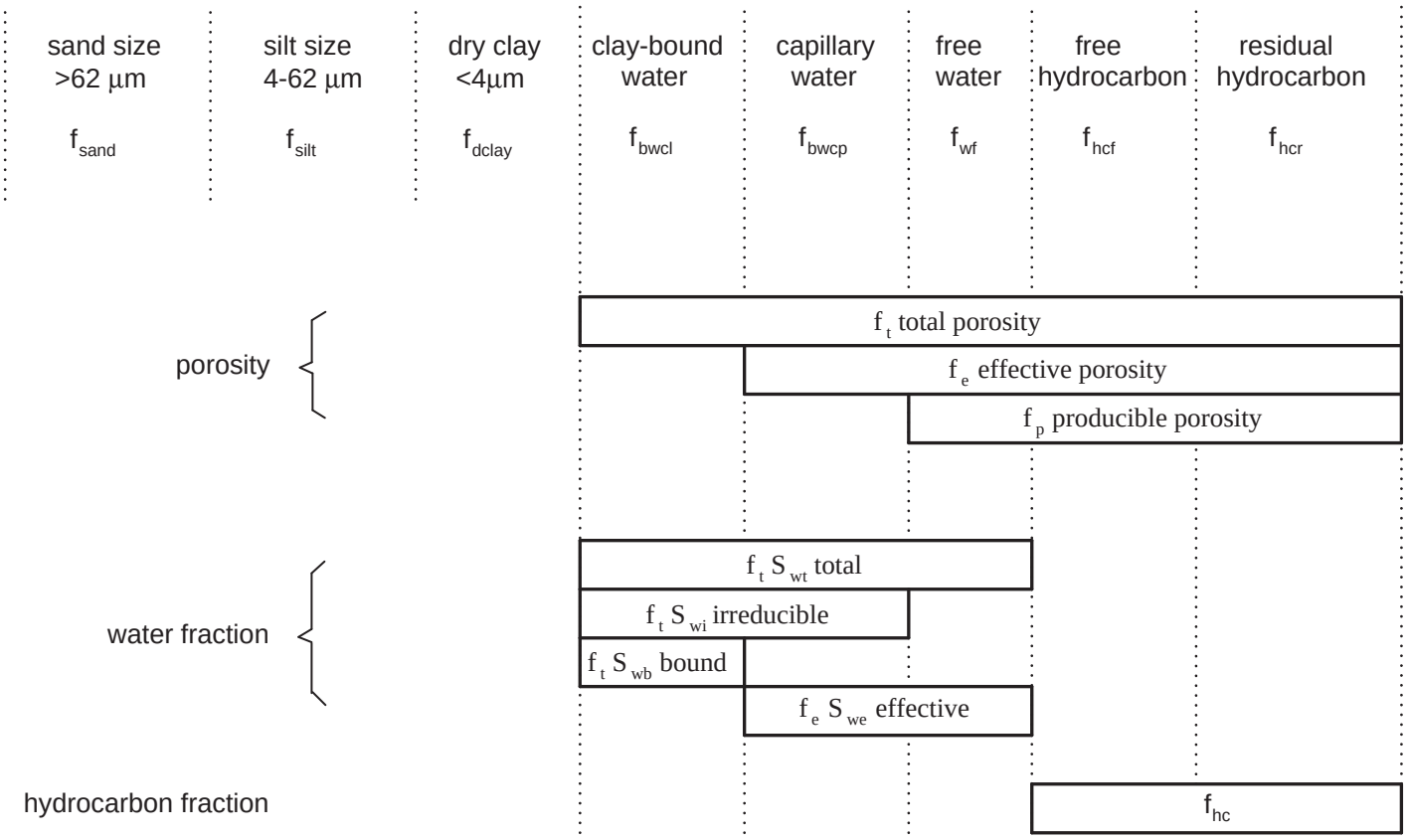

Figure PP7. Partitioning of a shaly sand into solid and pore space fractions. Pore space fractions are characterized by mobility of fluids. After Dodge, and others, 1996.

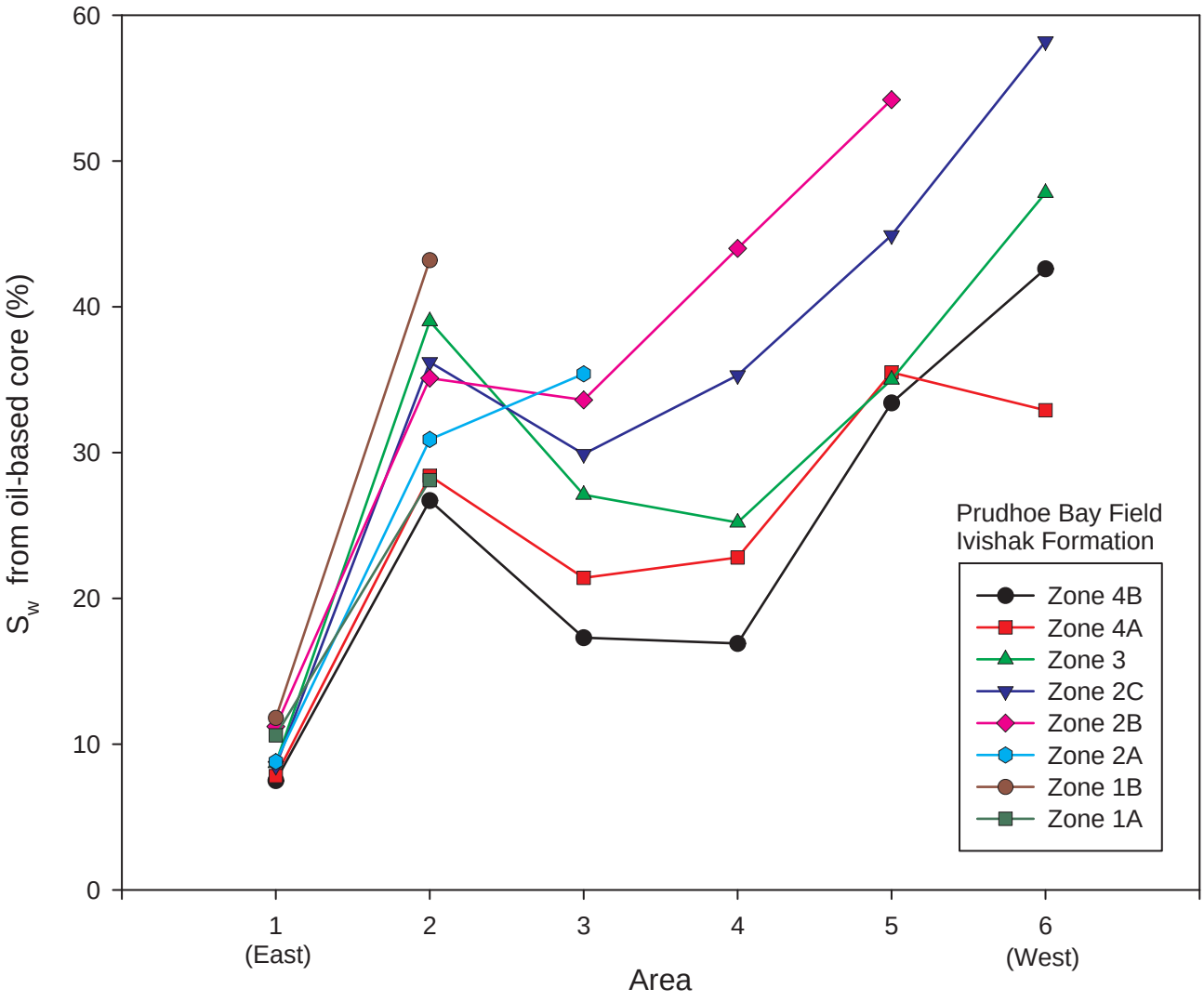

Figure PP8. Water saturation in Prudhoe Bay Field (Ivishak Formation) by area and zone. Area 1 lies updip in the northeast corner of the field. Zone 4B is uppermost stratigraphically. From Richardson and Holstein, 1994.

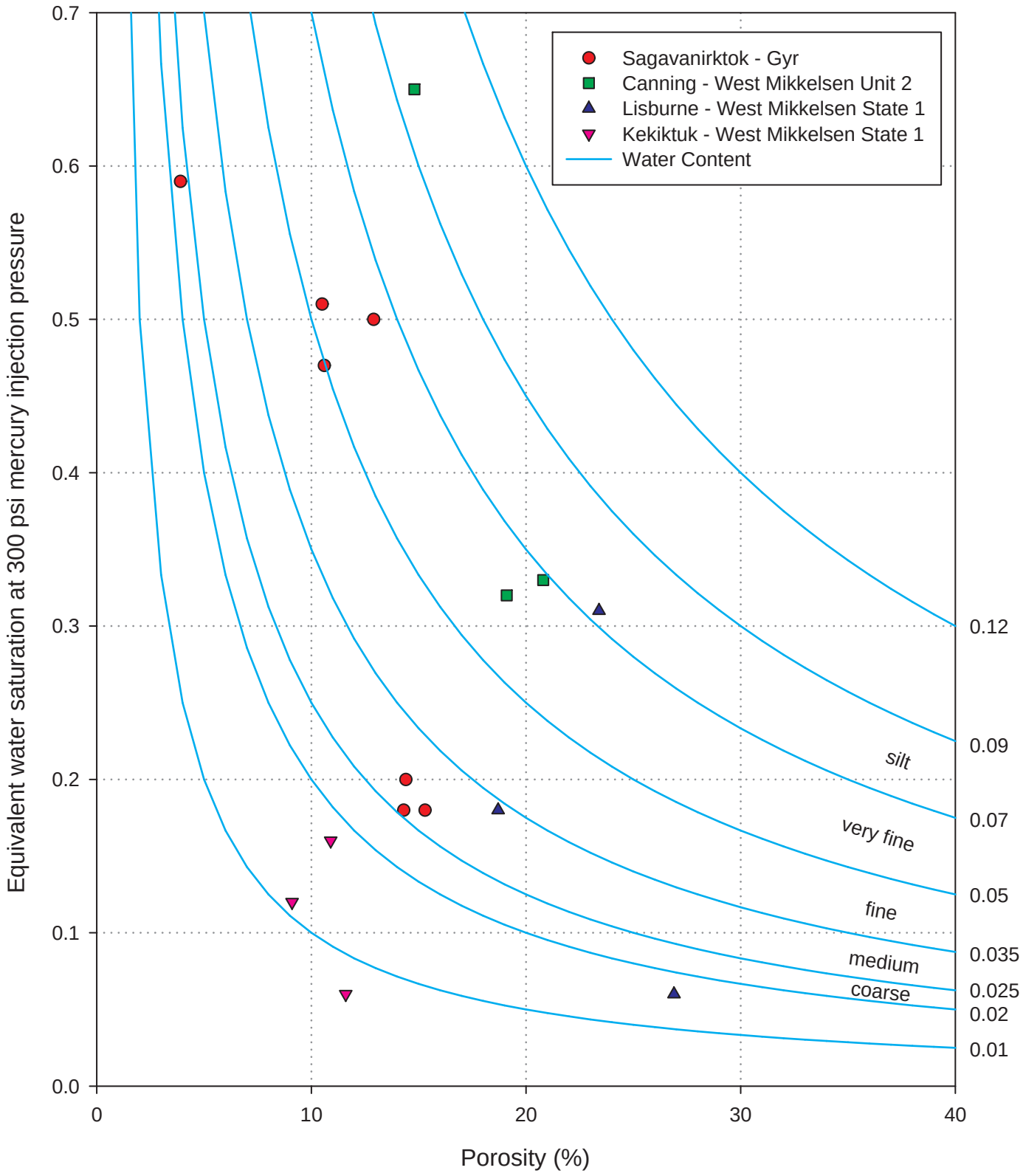

Figure PP9. Curves of constant volumetric water fraction, as given by the product of porosity times water saturation (given at right as decimal fraction). Data points for Lisburne, Kekiktuk, Canning, and Sagavanirktok Formations give equivalent water saturation from capillary pressure curves (Figs. PP6a, PP6b, PP6e, and PP6f) at 300 psi mercury injection pressure.

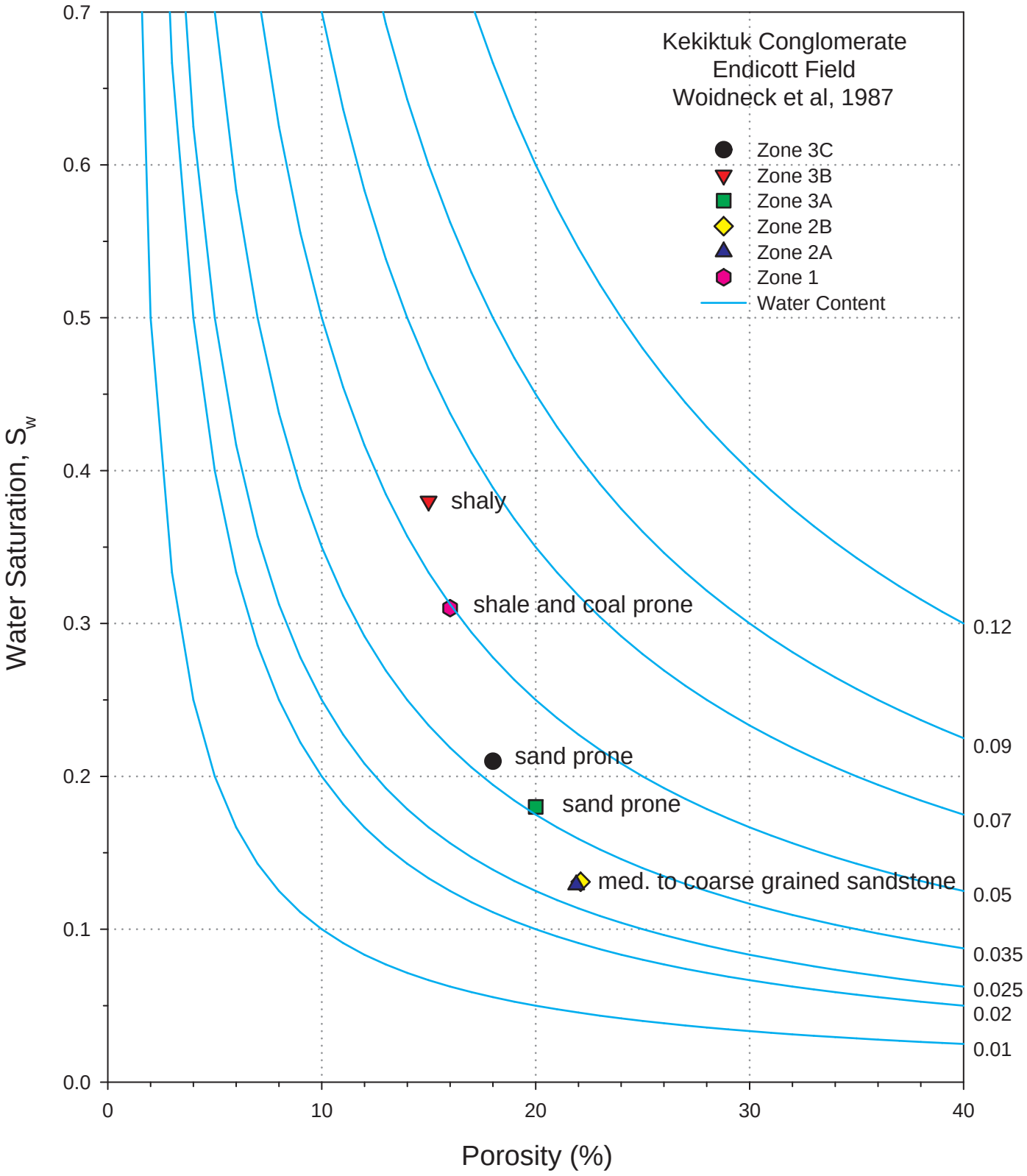

Figure PP10. Curves of constant volumetric water fraction, as given by the product of porosity times water saturation (given at right as decimal fraction). Data points are averages for the Kekiktuk Conglomerate in the Endicott Field (Table FP2).

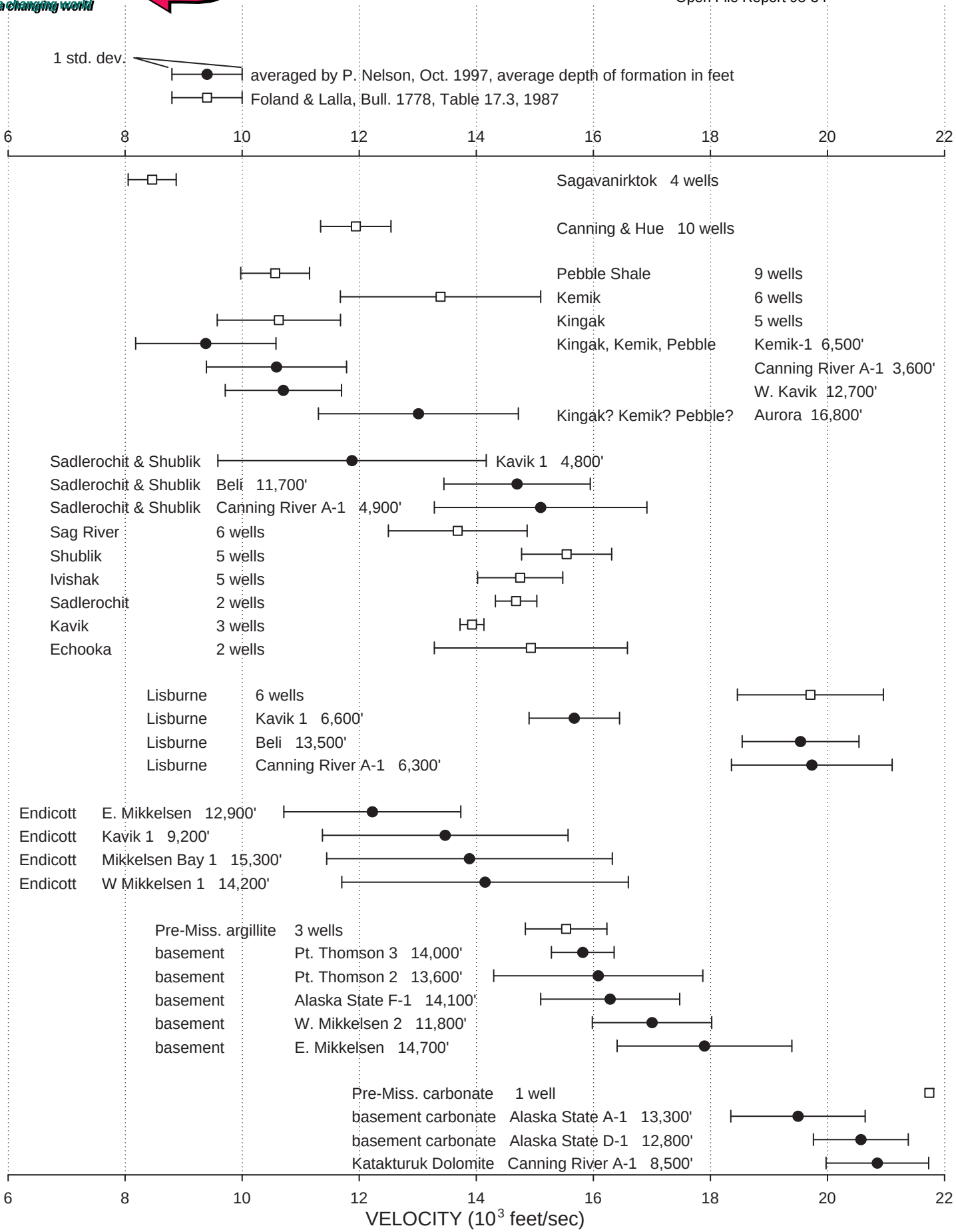

Figure PP11. Sonic velocities of individual formations, arranged in stratigraphic order, from sonic velocity logs. Data by Foland and Lalla, 1987, (open squares) are average values from several wells. Data from individual wells (black dots) are taken from Table PP8.

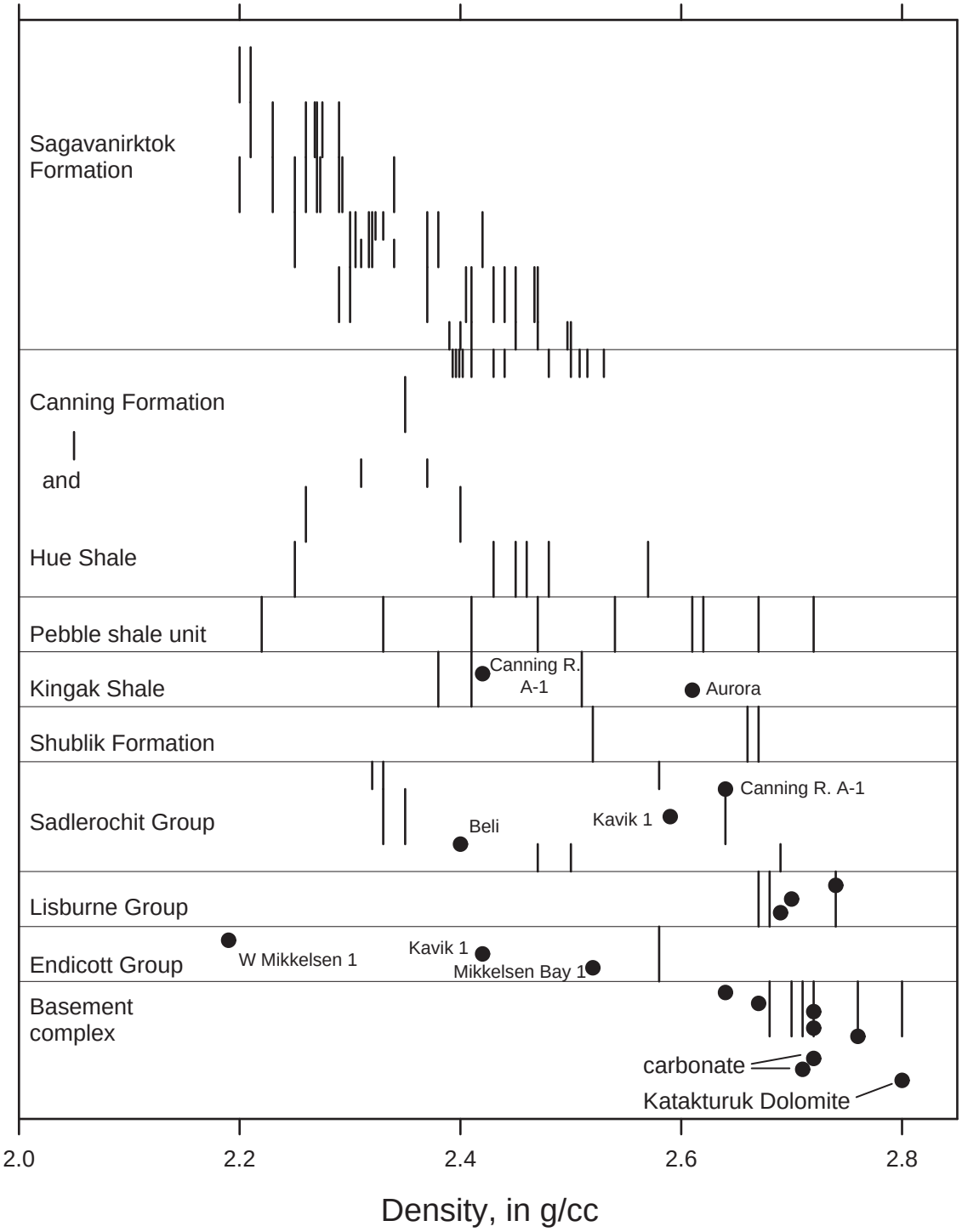

Figure PP12. Density values for individual formations from density logs. Vertical lines represent data by Robbins (1987). Black dots represent data from Table PP8.